UNIVERSIDADE DE COIMBRA

in collaboration with

UNIVERSITÀ DEGLI STUDI DI PADOVA

Assessment of cerebral hemodynamics by deconvolution methods in multiple sclerosis with DSC-MRI

Pedro Miguel Carvalho Figueiredo

Master's Degree in Biomedical Engineering

COIMBRA, SEPTEMBER 2011

UNIVERSIDADE DE COIMBRA

in collaboration with

UNIVERSITÀ DEGLI STUDI DI PADOVA

Assessment of cerebral hemodynamics by deconvolution methods in multiple sclerosis with DSC-MRI

Pedro Miguel Carvalho Figueiredo

Dissertation submitted for the degree of Master in

Biomedical Engineering

Jury

António Miguel Lino Santos Morgado

Miguel de Sá e Sousa de Castelo-Branco

Alessandra Bertoldo

Nicolás Francisco Lori

COIMBRA, SEPTEMBER 2011

Resumo

O presente trabalho foi desenvolvido numa colaboração entra a Universidade de Coimbra e a Universidade de Padova e tinha como objectivos principais o estudo da hemodinâmica do cérebro e de métodos de deconvolução para o estudo da mesma em esclerose múltipla com Contraste Dinâmico de Susceptibilidade (DSC) MRI.

Esclerose múltipla é uma doença que afecta muitas pessoas por todo o mundo. Ela é muito difícil de diagnosticar e é imprevisível, não só no ponto de partida mas também na maneira como se desenvolve.

Neste estudo três parâmetros hemodinâmicos vão ser estudados para se tentar uma melhor caracterização desta doença. No final vai ser possível descobrir que a hemodinâmica em esclerose múltipla tem diferentes valores, nomeadamente o Fluxo de Sangue Cerebral (CBF) e o Volume de Sangue Cerebral (CBV) na matéria cinzenta que se apresenta lesada vão ser mais pequenos do que na Matéria Cinzenta Aparentemente Normal (NAGM), contudo o terceiro parâmetro a Media do Tempo de Transição não vai sofrer diferenças estatísticas suficientes para se poder dizer que existem diferenças.

Também foi feito um estudo paralelo durante o processo e baseou-se na comparação de resultados entre a Decomposição de Valor Singular (SVD) e Decomposição de Valor Singular com Bloco Circulante (cSVD). No final não foram encontradas diferenças significativas sendo a diferença maior a dispersão era menor para a Decomposição de Valor Singular com Bloco Circulante.

Mais estudos precisam de ser feito nesta área por causa da natureza da doença. Significando que conhecer porquê, onde, quando e como se manifesta e como se desenvolve vão ser passos cruciais na compreensão da doença.

Palavras chave: esclerose múltipla, DSC-MRI, SVD, cSVD, CBF, CBV, MTT

Abstract

The present research has been developed in collaboration between the University of Coimbra and the University of Padua and has as its main goals the study of the brain hemodynamics and the deconvolution methods of assessing them in multiple sclerosis with Dynamic Susceptibility Contrast (DSC) -MRI.

Multiple sclerosis (MS) is a disease that affects many people around the world. It is difficult to diagnose and it is unpredictable not only in its initial stages but also in the way it develops.

In this work three more parameters will be studied to attempt a better characterization of this disease in the end it will be found that hemodynamics in a multiple sclerosis patient have different values, namely the Cerebral Blood flow (CBF) and Cerebral Blood Volume (CBV) in grey matter with lesion will be smaller than in apparently Normal grey matter (NAGM), however Mean Transit Time (MTT) will not suffer enough statistical differences to be consider different.

Another parallel study was made during the process and it was based on the results comparison between Singular Value Decomposition (SVD) and Block Circulant Singular Value Decomposition (cSVD). In the end no big differences between them were found and the major one was that the dispersion for Block Circulant Singular Value Decomposition where smaller.

More studies need to be done in this area because of the nature of the disease. Meaning that understand why, where, when and how it manifests itself and how it develops will be crucial steps in the comprehension of the disease.

Keywords: multiple sclerosis, DSC-MRI, SVD, cSVD, CBF, CBV, MTT

Contents

Table of contents

Abbreviations

Abbreviation	*meaning*
AIF	Arterial Input Function
AUC	Area Under the Curve
ASL	Arterial Spin Labelling
BBB	Blood Brain Barrier
CASL	Continuous ASL
CBF	Cerebral Blood Flow
CBV	Cerebral Blood Volume
CNR	Contrast to Noise Ratio
CPV	Cerebral Plasma Volume
CRCV	Cerebral Red Cell Volume
cSVD	Block Circulant Singular Value Decomposition
DSC	Dynamic Susceptibility Contrast
EDSS	Expanded Disability Status Scale
EPI	Echo Planar Imaging
EPISTAR	Echo Planar Imaging and Signal Targeting with Alternating Radiofrequency
FAIR	Flow Alternating Inversion Recovery)
FID	Free Induction Decay
FOV	Field Of View
GE	Gradient-Echo
GM	Gray Matter
MatLab	Matrix Laboratory
MR	Magnetic Resonance
MRI	Magnetic Resonance Imaging
MS	Multiple Sclerosis

MTT	Mean Transit Time
NAGM	Normal Appearing Gray Matter
NMR	Nuclear Magnetic Resonance
PASL	Pulsed ASL
PET	Positron Emission Tomography
QUIPSS II	Quantitative Imaging of Perfusion Using a Single Subtraction
ROI	Region of Interest
RRMS	Relapsing-remitting
SD	Standard Deviation
SE	Spin-Echo
SNR	Signal to Noise Ratio
SPM	Statistical Parametric Mapping
SVD	Singular Value Decomposition
TE	Echo Time
TI	**I**nversion Delay
TR	Repetition Time
TTP	Time to Peak
VOI	Voxel of Interest
WM	White Matter

List of figures

List of tables

1. Introduction

1. Multiple sclerosis

Multiple sclerosis (MS) is a demyelination disease of the central nervous system that affects mainly young adults, generally between 15 and 40 years old, with average at 30 years old, has a frequency between 2 and 150 per 100,000 depending on the population characteristics, without a previous pathological state preferential in women in zones with a temperate climate [10][11][15].

Furthermore some studies have found that the susceptibility for multiple sclerosis can be affected by other factors like the childhood environment and genetic factors, once the disease has greater incidence in urban zones, higher socio-economic groups and white people [10][11].

The trigger for this disease in not yet well known but seems to be associated with immunological deregulation that occurs in a person with genetic predisposition. Besides viral infections usually proceed an MS attack, suggesting that anti-viral defense cause an autoimmune response resulting in perivascular inflammation of the CNS and demyelination [10].

Myelin destruction occurs when T lymphocytes release interferon. This happens when the infecting agent carries the antigen that mimics the myelin autoantigen generating a striking response to oligodendrocytes [10].

Macrophages after the agent process presents on their surface viral antigens with HLA molecules namely from DR2 class [12] [13]. From this combination can result a similar complex to autoantigen of myelin, and in this point the genetic predisposition plays the role, once, this predisposition is related to the composition of HLA DR2 in other words it gives the similarity between HLA-Viral Antigen and autoantigen.

If the person presents this genetic predisposition, after the viral infection, the immune response follows its normal path in the beginning, but after the connection of T lymphocytes with HLA-antigen it will promote their activation and proliferation.

These cells will mediate attacks to all cells with this antigen presents in the surface. Some of them will adhere to the blood brain barrier (BBB) releasing interferon-gamma and lymphotoxin facilitating the adhesion of more and more T lymphocytes to the BBB [13].

This process will break the BBB allowing the T lymphocytes to get in the CNS. Inside of CNS, microglial cells more precisely oligodendrocytes will exhibit the antigen.

The T lymphocytes will connect with the oligodendrocytes suffering the secondary activation proliferating even more and release more cytokines.

Cytokines will enhance the presentation of antigens by microglial cells and will stimulate macrophages to produce tumor necrosis factor-alpha (THF). All this inflammatory process will add more damage to BBB allowing more T lymphocytes, macrophages, B lymphocytes, antibodies and complement to cross this barrier.

Meanwhile T lymphocytes stimulate B lymphocytes to produce antibodies which will link to oligodendrocytes and to myelin attracting activated macrophages. Those will attack the myelin barrier and release tumor necrosis factor which will in turn attack the oligodendrocytes.

Additionally those antibodies already linked to myelin will attract and activate the complement which will create three kinds of fragments. Those fragments will damage BBB, attract more macrophages, and poison oligodendrocytes. This process will add continuously damage to the myelin [13].

The degeneration of myelin causes the reduction or signal loss in some nerves resulting in a big variability of symptoms depending on the place and on the amount of damage.

When the damage is minor the myelin layer can keep the dielectric properties and the signal is not affected, exceptionally in some cases when the temperature rises.

However over a certain amount of damage the axon will not be prepared to work, because it will have a deficit of potassium channels in areas of Ranvier nodes, not allowing the signal to pass through.

At this point multiple sclerosis starts having some symptoms, which are quite ambiguous and to a certain extent difficult to associate with the disease, sometimes in the beginning patients are diagnosed as neurotic or hypochondriac.

During a neurological exam if there are some suspicions of multiple sclerosis some symptoms should be taken in to account specially coordination, balance, lack of strength, reflexes and alterations on ocular movements, on speech, on verbal articulation or on sensitivity.

Still all these symptoms can be related with different diseases leading to some errors and some miss-understanding over the final analysis. Some complementary tests can be made like the study of evoked potential and lumbar puncture.

In this field magnetic resonance is starting to be very important since with this technique it is possible to characterize the number, size and distribution of the damage.

After a suspicion of multiple sclerosis the disease will not be easy to confirm and to help in this process some norms have been created first neurologists use the Schumacher criteria [Schumacher et al, 1965] where some points need to be field, after this one Poser criteria [Poser, 1983] have be accepted as update; many work has been done and some other criteria can be found nowadays like those proposed by McDonald et al, 2001 and Polman et al, 2005.

Furthermore ME is a very peculiar disease giving lots of problems for those who try to characterize it; from this point of view it can be characterized in many ways but first will be explain the way that did not regards an exact point in time but regards the kind of evolution expressed; there are four approximations (figure1.1).

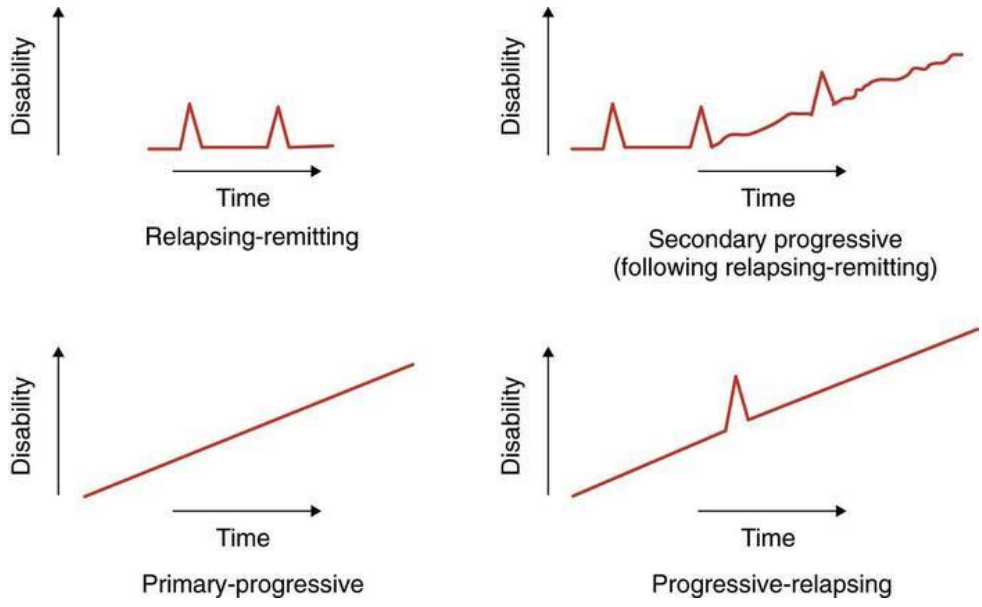

Figure 1.1 types of multiple sclerosis [35].

Relapsing-remitting where the symptoms appear and disappear spontaneously over time, this is the most common type. Secondary progressive MS is taken as the development of Relapsing- remitting when irreversible injuries can no longer be compensated by the nervous system. Primary progressive when patient gradually get worse, without clinical relapses. Progressive relapsing when patient gradually get worse but this time with relapses that appear and disappear spontaneously, can represent Secondary progressive MS in an initial phase[35].

ME characterization is very important for prognosis and therapeutic decisions.

ME can also be characterized by the patient disability status. And for that will be used the Expanded Disability Status Scale (EDSS) created by Kurtzke 1983 where lower values represent people with low disabilities on Functional Systems and big values for those with big disabilities.

Table 1.1 Expanded Disability Status Scale (EDSS) extracted from ref [21].

0.0	Normal neurological examination
1.0	No disability, minimal signs in one FS
1.5	No disability, minimal signs in more than one FS
2.0	Minimal disability in one FS
2.5	Mild disability in one FS or minimal disability in two FS
3.0	Moderate disability in one FS, or mild disability in three or four FS. Fully ambulatory
3.5	Fully ambulatory but with moderate disability in one FS and more than minimal disability in several others
4.0	Fully ambulatory without aid, self-sufficient, up and about some 12 hours a day despite relatively severe disability; able to walk without aid or rest some 500 meters
4.5	Fully ambulatory without aid, up and about much of the day, able to work a full day, may otherwise have some limitation of full activity or require minimal assistance; characterized by relatively severe disability; able to walk without aid or rest some 300 meters.
5.0	Ambulatory without aid or rest for about 200 meters; disability severe enough to impair full daily activities (work a full day without special provisions)
5.5	Ambulatory without aid or rest for about 100 meters; disability severe enough to preclude full daily activities
6.0	Intermittent or unilateral constant assistance (cane, crutch, brace) required to walk about 100 meters with or without resting
6.5	Constant bilateral assistance (canes, crutches, braces) required to walk about 20 meters without resting

7.0	Unable to walk beyond approximately five meters even with aid, essentially restricted to wheelchair; wheels self in standard wheelchair and transfers alone; up and about in wheelchair some 12 hours a day
7.5	Unable to take more than a few steps; restricted to wheelchair; may need aid in transfer; wheels self but cannot carry on in standard wheelchair a full day; May require motorized wheelchair
8.0	Essentially restricted to bed or chair or perambulated in wheelchair, but may be out of bed itself much of the day; retains many self-care functions; generally has effective use of arms
8.5	Essentially restricted to bed much of day; has some effective use of arms retains some self-care functions
9.0	Confined to bed; can still communicate and eat.
9.5	Totally helpless bed patient; unable to communicate effectively or eat/swallow
10.0	Death due to MS

This is a progressive disease that strikes in many fields and the point of discover is really important, so important or even more is the reason why the lesions start. Those two are the biggest problems in this are because if they become possible to estimate the lesion will be detected in the earlier fazes when the tissue has no permanent damage.

2. Image techniques to evaluate brain hemodynamics

For noninvasive assessment of brain hemodynamics, in vivo, a good understanding of the brain is very important and this means understanding the brain in a normal and in a pathological state.

1.2.1. MRI

In the last decade huge progress has been made in the macroscopic image of human brain activity and in this field we can highlight the Magnetic Resonance Imaging (MRI). Thanks to the high levels of temporal and special resolution without ionizing radiations this technique is becoming more and more a valid alternative to PET.

Positron emission tomography (PET) is a powerful tool in this field because it can measure cerebral blood flow (CBF) and cerebral blood volume (CBV), by the interpretation of a tracer

activity. This means that PET creates good quantifications for CBF and CBV, making it the gold-standard of quantitative imaging technique.

However PET has some limitations like injection of radioactivity tracers or the request of arterial sampling.

Being more precise the Dynamic Susceptibility Contrast- Magnetic Resonance Imaging (DSC-MRI) is the most interesting for the quantitative studies of the brain hemodynamics even in pathological states.

This technique is based in the injection of paramagnetic contrast agent in a peripheral vein. When the bolus of contrasting agent reaches the region of interest it perturbs the total magnetic field decreasing the relaxation time constants and influencing the detections.

The sensitive imaging sequence can be traced using T_2 or T_2*(T1 and T2 are intrinsic properties of the tissues and T2* depends on inhomogeneity of the magnetic field) relaxation times resulting from the passage of the bolus on the place of interest.

Furthermore the Magnetic Resonance Imaging can be performed using either Spin Echo (SE) or Gradient Echo (GE) sequences, but the higher sensitivity of T2* to DSC make GE the preferable choice, and GE can reflect the signal from most of the large vessels .

So the analysis of the time progress of bolus passage allows the measurement of cerebral profusion. This technique has been developed over more than 20 years in order to allow better measurements of CBF, CBV and MTT.

1.3.Objectives

This work results from the cooperation between the University of Coimbra and the University of Padua with supervising of Professor Alessandra Bertoldo from University of Padua and Professor Miguel Castelo Branco from the University of Coimbra.

The main goal was to study the hemodynamics of the brain in a cortical lesion with Dynamic Susceptibility Contrast agent. This was not a work started from the ground point; the group connected to the Department of information engineering had already done some studies on Dynamic Susceptibility Contrast – Magnetic Resonance Imaging (DSC-MRI).

More precisely the objective was to study the:

- Procedure to the quantization of the brain hemodynamics from DSC-MRI data.
    - Analysis of two different procedures to deconvolution: Singular Value Decomposition and block-Circulant Singular Value Decomposition.
- Statistical analysis of the brain hemodynamic in the grey matter of a MS lesion.

2. Theory

2.1.Basics of NMR

NMR suggests the interaction between a magnetic field and an atomic nuclei, but not all of the compounds can be used with this technique only those who manifest magnetization, more precisely ^{13}Carbon, ^{12}Nitrogen, ^{19}flourine,^{23} sodium,^{31}phosphorus and ^{1}hydrogen nuclei.

All those nuclei have something in common, they possess a special internal angular momentum called spin. The spin is intrinsic to the nuclei and is generated by the rotatory motion of the particles around its own axis which creates small magnetic fields.

This can be quantified taking the value of zero, a whole number or a half integer. Still only those who possess whole or half integer spin values can be used in NMR because only those magnetic fields can be combined with an external magnetic field aligning the proton.

The hydrogen nucleus has a great importance because it is extremely common in common water and fat and is composed by of one proton and one electron. Possessing only one proton it can have only one spin number of 1/2 and can take only two possible energy states (-1/2 and 1/2).

However if on one hand there is no magnetic field applied, the magnetic moments will have random directions and the resulting force will be nil. In the other hand if the nuclei are under a certain magnetic field B_0, they will align their magnetic moments and get arranged by B_0 orientation.

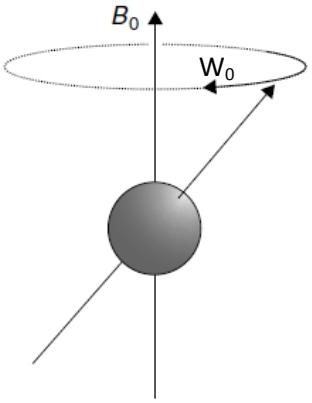

Figure 2.1 Schematic representation of a proton spinning on his own axis but under the influence of the field B_0 [26].

So it can be said that magnetic moment related to a spinning nuclei will couple with B_0 more precisely every nuclei will be able to dispose in two different directions the main field direction (low-energy state) or against the field direction (high-energy direction) Figure [2.3], [26].

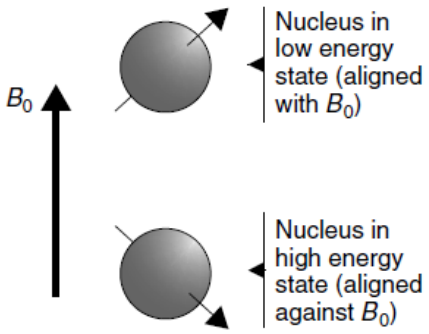

Figure 2.2 Possible angles of orientation for a hydrogen atom [26]

The force experienced by the nuclei will make it move into the field direction with a characteristic frequency known as the *Larmor* frequency (v_0) (equation 2).

$$W_0 = \gamma B_0 \tag{1}$$

Where γ is the gyromagnetic radio (for hydrogen will be 2.68x10^8 rad s^{-1} T^{-1}) and the angular velocity W_0 will be dependent on B_0 however in almost MR systems it can have a cyclic frequency range (equation [2]) between 0.3 and 300 MH [26].

$$v_0 = w_0/2\pi$$

(2)

Still the spin phase will be random meaning that this effect has to be seen not in an individual way but in a way where all the materials are a big group of nuclei expose to the same magnetic field.

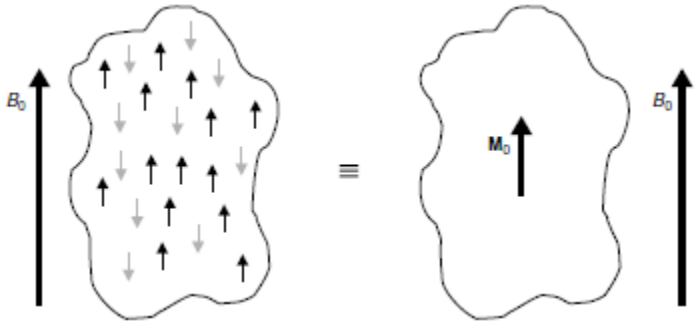

Figure 2.3 Individual magnetization and sum of all magnetizations. It can be seen that will exist more low-energy alignments generating a macroscopic magnetic field (M_0) in B0 direction [26]

This group of nuclei will split into two groups one for those who align with the field and the other which will align against the field, this distribution is related to thermal agitations which at room temperature will favor the low energy state (field direction) but only for a small amount. If we take into account that the difference of energy between the levels is very small the final energy of the sample will be small to.

This difference between populations can be explained by the Boltzmann distribution:

$$\frac{n^-}{n^+} = e^{-(\Delta E/KT)}$$

(3)

Where n^- and n^+ represents the two populations with different energies, high energy and low energy respectively, ΔE is the energy difference among the possible states of the nuclei, K is the Boltzmann constant (k = 1,3805 x 10^{-23}J/Kelvin) and T is the temperature in kelvin.

If we take in account that:

$$\Delta E = h v_0$$

If $w_0 = 2\pi . v_0$

$$= \frac{h w_0}{2\pi}$$

$$= \hbar \boldsymbol{\gamma B_0} \quad \textbf{(4)}$$

Where h is the Plank constant (h= 6,626x10^{-34} J s) and ħ =$h/2\pi$, then

$$\frac{n^-}{n^+} = e^{-(\hbar \gamma B_0 / KT)}$$

So taking in account that ΔE is near 10^{-26} and KT around 10^{-24} can be conclude that the relation between n^- and n^+ will be a little bit lower than one favoring the low-energy state at room temperature. However this relation can be changed because it shows dependency on the magnetic field, B_0, and the temperature, T, both in different parts on the equation meaning this that it will increase with B_0 and decrease with T.

2.2.Magnetic Disruption and relaxation

Let us consider that B_0 will be in the direction of z axis, and there is no disruption on the system so the resulting magnetization (M_0) will be in the same direction, meaning that in this situation the longitudinal magnetization (M_z) will be equal to M_0.

However, it is possible to change the magnetization vector from its stable position for that a magnetic field (B_1) needs to be added. If B_1 is perpendicular to B_0 and has an oscillation at Larmour frequency (v_0) will be produced one effect of resonance.

This effect is only possible because the atoms can absorb the frequency making them pass to a level of superior energy, so for each rotation M_y will move more and more away from z axis, in other words this behavior will change the relation of $\frac{n^-}{n^+}$ taking it to one, not because those atoms in a low-energy state change to a high energy state but because the component in z starts to disappear and component in the XY plane start to appear.

If a 90° pulse is applied the longitudinal component (M_z) will disappear and the transvers component (m_{xy}) will became positive.

After this, the pulse will be turned off and the system will make everything to come back to the initial stable point and for that will be needed to release the energy absorbed by the atoms, this energy decay will create a NMR signal than can be measured and is called Free indication decay (FID) .

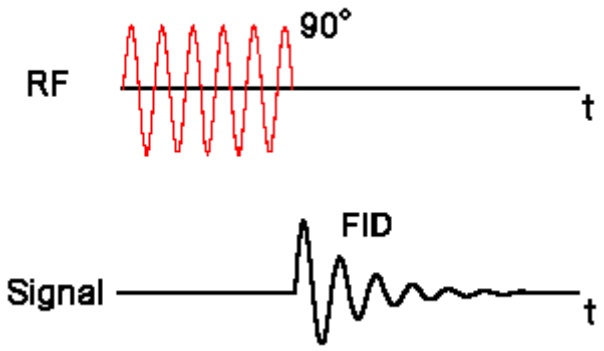

Figure 2.4 Schematic representation of the influence of radio frequency and his FID [30]

This signal can be analyzed in to different ways by the longitudinal component or the transvers component.

If on one hand is studied the growing of M_z by:

$$M_z = M_0(1 - e^{-\frac{t}{T_1}}) \quad \textbf{(5)}$$

Where T_1 is called longitudinal relaxation time and is the time needed to M_z return to 63% of his maximum value.

On the other hand is studied the decrease of M_{xy}

$$M_{XY} = M_{XY0}.e^{-\frac{t}{T_2}} \quad \textbf{(6)}$$

These represent the return to the initial stability and the constant of time which represents this transformation is called relaxation spin-spin or T_2 (transverse relaxation).

In all the cases T_2 will be always smaller than T_1, due to the fact that T_1 is a positive exponential and T_2 is a negative exponential and both values depend on where the 63% of the maximum maximization is reached.

Furthermore, this relaxation has its name because it results from the interaction between spins, this interaction is created by the disorganization of the spins due to small heterogeneities present in the magnetic field, B_0, these two things are what influence the relaxation time.

So if we have a really stable magnetic field the resulting time constant will be pure T_2. But if instead a non-stable magnetic field is applied the resulting time constant will not be T_2 but T_2*:

$$\frac{1}{T_2^*} = \frac{1}{T_2} + \frac{1}{T_{2\ non\ stable}} = \frac{1}{T_2} + \frac{\gamma \Delta B_0}{2} \quad \textbf{(7)}$$

T_2* will be defined as the time that signal needs to reach 63% of its maximum value and will be always lower than T_2.

2.3.RMN signal extraction

Before beginning it should be known that the signal is captured by a bobbin in the XY plane, this signal will be extracted from a piece of tissue meaning that if this tissue is from a human body it will have many variables (proton density, T_1 and T_2) that will distinguish him from the tissue immediately after.

This will allow the creation of an image because if every piece is so small that it can be associated to a pixel the resulting signal from every piece will build that image.

However there is more than one way to extract this information. Spin-Echo (SE) and Gradient-Echo (GE) are two fast sequences able do what is proposed in this paper, in this case they are two methods of tracking a bolus injection.

- **Spin-Echo**

In this case transverse magnetization will be generated by the application of a radio frequency pulse of $90^0_{x,y}$, logically will be expected that after it the material transverse magnetization gets dephased, meaning that no pulse can be applied and no new FID could be generated.

The new pulse has to wait until everything becomes stable once more, so all the process became possible; this could take some seconds.

Still it is not necessary to wait all that time if another pulse of 180^o is applied after a time TE/2, this new pulse will realign the spins at a time TE creating one echo and making the atoms ready for a new pulse.

TE is called Echo-time and will be the time between the 90^o RF pulse and the maximum value of the echo received.

In this technique a long Repetition time (TR – time between two successive pulses of 90^0) will give better results because in this case all atoms are at the desired frequency and ready to the next pulse, if this time is reduced and becomes smaller than some of the T_1's of the tissue, the frequencies will not be the desired one and the signal will be weaker.

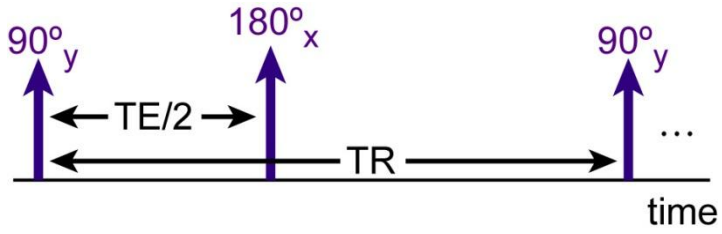

Figure 2.5 Spin-Echo pulses (90^0 and 180^0).

- **Gradient-Echo**

This technique born to reduce the time at all cost and in this case the cost is the signal intensity. Thus will have its base in the appliance of a transverse magnetization generated by the application of a radio frequency pulse with a flip angle from 90^0 to 10^0, making M_z to reach stability faster.

In this case the flip angle will be the one controlling the speed acquisition and the image quality because if one get better the other gets worse.

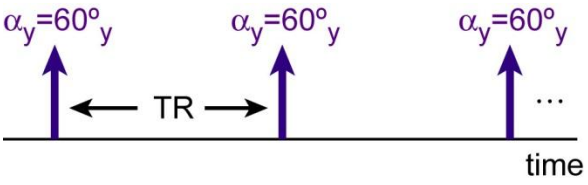

Figure 2.6 schematic representation of Gradient-Echo at angle of 60^0.

2.4.Dynamic Susceptibility Contrast (DSC)-MRI

DSC-MRI is based in the injection of a tracer and proves itself to be a great discovery once with the new image techniques it is possible to obtain good maps of cerebral perfusion. Usually, an injection of a high concentrated tracer is given to the patient and the MR signal is measured when the tracer passes through the brain.

A typical paramagnetic tracer is Gadolinium Gd-DTPA (fig. 2.7), because this substance has properties that will change the intrinsic nuclear MR properties of the tissues by generating a strong local magnetic field.

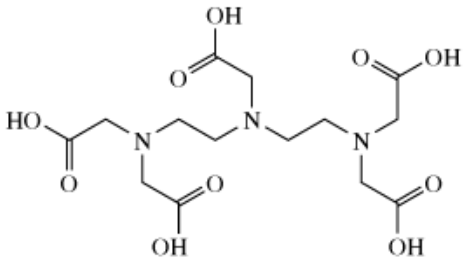

Figure 2.7 gadolinium Gd-DTPA

Consequently the tissue will experience a new internal magnetic field which depends on the strength of magnet and the tissue properties resulting in a magnetic field that can be described as

$$B_{int} = B_0(1 + x) \quad \textbf{(8)}$$

B_0 is the magnetic field applied and x is the magnetic susceptibility of the material. This last one will be directly proportional to the concentration of the agent. For parametric materials, x

has positive values that increase the internal field aligning the molecules this means that tissue susceptibility will change in a way that can be measured.

These changes will cause the loss of signal because parametric field will generate magnetic inhomogeneities thus de-phasing the transverse magnetization of the surrounding tissues.

To detect all the developments during the bolus injection a really fast process will be needed, DE and GE have some differences.

DE is heavily influenced by capillary bed but it can give in some cases such as the study of specific regions like temporal lobes or frontal sinus a better image.

GE on the other side is influenced hugely by information related to large vessels (≈20µm diameter). The GE will be selected to this work because of its higher sensitivity to T_2* which is the more influenced by the contrast agent.

Some protocols can be made to this procedure but a typical protocol is base in a single acquisition after a GE sequence shot with TE between 40 and 60 ms, TR between 800 and 1200 ms and a 1.5T magnetic field. Flip-angle between 60 and 80^{o} is chosen to maximize the signal to noise ratio (SNR) and to minimize the noise that can come from any T_1 weighing.

2.5.Considerations

DSC-MRI images are based on the principles of tracer kinetics for non-diffusible tracers called Dilution Theory [Zierler K.L., CR 10, 1962; Zierler K.L., CR 16, 1965; Axel L. Radiology 137, 1980].

This means that the following assumptions are true:

Contrast agent is non-diffusible;

Recirculation of the tracer does not exist;

The blood flow is constant (only a stationary blood flow can be measured, this means that there's only one value of flow per experiment; still the flow oscillations are not big enough if we take in to account the experiment time);

The contrast agent does not perturb the system

The blood-brain barrier (BBB) is undamaged confining the contrast agent to the intravascular space.

So under these assumptions, some parameters can be estimated like Cerebral Blood Volume (CBV), Cerebral Blood Flow (CBF), Mean Transit Time (MTT) and Residue function (R(t)).

3. Math

3.1.Reality

The signal from the DSC-MRI is affected by the amount of contrast agent present within a voxel by perturbing the magnetic field. Then the relaxation time is changed modifying the T_2*. This signal is called weighted signal, S(t).

$$S(t) = S_0 e^{-\Delta R_2{}^*(t).TE} \tag{9}$$

$$\Delta \mathrm{R}_2 = R_2^*(t) - R_2^*(0)$$

Where S(t) is the signal value from water protons at time t and if t=0, S_0 is the signal value before bolus injection, T_E is the repetition time and ΔR_2 is the change in transverse relaxation rate where

$$R_2^*(t) = 1/T_2^*(t) \tag{10}$$

Assuming a linear relationship between the change in transverse relation rate R_2* and the parametric concentration of tracer C_{VOI}(t) inside the voxel, the alteration in concentrations over time during the passage of contrast agent in a VOI can be characterized as:

$$C_{VOI}(t) = k_{VOI} \Delta R_2{}^*(t) \tag{11}$$

Where K_{VOI} is an unknowing constant that depends on the tissue, the contrast agent, the field strength, and the pulse sequence properties, for his complexity and difficulty of calculation for each voxel, is assumed the same constant, K= K_{VOI} for both tissue and arterial concentration. And in many cases this constant can be taken as 1 which will introduce some errors.

From the equations 9 and 11:

$$C_{VOI}(t) = -\frac{k_{VOI}}{T_E}\ln\left(\frac{S(t)}{S_0}\right)$$

(12)

This equation is fundamental for DSC-MRI, since this formula provides each voxel with a concentration.

3.2.Theory

The residue function describes the fraction of tracer present in the VOI at time **t** after the bolus injection.

Residue function is a decreasing function in the time and for t=0 a R (0) =1 is assumed in other words a unitary bolus injection is assumed, this means that:

$$\int_0^\infty h(\tau)d\tau = 1$$

(13)

Transport function, h (t), is a characteristic of the system, dependent mainly from the flow and the vascular structure of the volume of interest and define the probability density function of passage through the VOI

If the bolus amplitude of the tracer is q_0 in the initial moment (t=0), the amount of tracer leaving the VOI is:

$$q_{out} = q_0 \int_0^t h(\tau)d\tau$$

(14)

Knowing the amount of tracer that leaves the VOI the quantity still remaining in VOI is:

$$q_{in}(t) = q_0 - q_0 \int_0^t h(\tau)d\tau = q_0 \left[1 - \int_0^t h(\tau)d\tau\right]$$

(15)

The residue function is given by

$$R(t) = 1 - \int_0^t h(\tau)d\tau$$

(16)

Residue function works on the assumption of an ideal bolus injection, meaning that at time t=0 all the bolus is in the VOI.

So the residue function can describe the whole system, however residue function is dependent from the arterial input function (AIF).

The Arterial Input Function is the concentration of tracer entering the tissue of interest at a time t from the signal changes in the major artery.

After this and in case of an intact BBB, the Central Blood Volume (CBV) can be determined from the ratio between the areas under the concentration time curve of the tracer of a certain VOI ($C_{VOI}(t)$)and the concentration time curve of the tracer in the feeding vessel of a certain VOI ($C_{AIF}(t)$).

The normalization of CBV to the density of the brain (ρ) will be given by [3]:

$$CBV = \frac{k_h \int_0^\infty C_{VOI}(\tau)d\tau}{\rho \int_0^\infty C_{AIF}(\tau)d\tau}$$

(17)

Where K_H denotes the difference in hematocrit (H) between large (0.45) and small vessels (0.25) [1], for the reason that the plasma is the only place where the tracer can be.

$$k_H = \frac{1 - H_{lv}}{1 - H_{sv}}$$

(18)

CBF results from the addition of Cerebral Plasma Volume (CPV) to the Cerebral Red Cell Volume (CRCV). Once the hematocrit is defined as H=100.CRCV/CBV, the CBV=CPV+H.CBV=CPV/(1-H).

By the definition of CBV:

$$CBV = \frac{amount\ of\ blood\ in\ a\ VOI}{\rho\ .\ area\ under\ the\ blood\ input\ curve}$$

$$= \frac{1}{\rho}\frac{1 - H_{Lv}}{area\ under\ the\ plasma\ input\ curve}\frac{amount\ of\ plasma\ in\ a\ VOI}{(1 - H_{Sv})} \quad \textbf{(19)}$$

$$= \frac{1 - H_{Lv}}{\rho(1 - H_{Sv})}\frac{\int_0^\infty C_{VOI}(\tau)d\tau}{\int_0^\infty C_{AIF}(\tau)d\tau}$$

The CBV units are commonly given in milliliters per 100 grams of tissue (ml/100g) or microliters per gram (µl/g).

In this comparison one more parameter needs to be taken into account, a parameter called Mean Transition Time (MTT) and represents the average time that a particle of tracer takes to pass thought the VOI. In other words MTT is the center of mass of the distribution h (t):

$$MTT = \frac{\int_0^\infty t.h(\tau)d\tau}{\int_0^\infty h(\tau)d\tau} \quad \textbf{(20)}$$

From the equation 13 and 16:

$$MTT = \int_0^\infty t.h(\tau)d\tau = \int_0^\infty R(\tau)d\tau \quad \textbf{(21)}$$

However there is a different way to calculate de MTT value. This way is based on the theorem of central volume of the indicator Dilution Theory [Axel L., Radiology 137, 1980; Stewart G.N. JP 15, 1984; Meier P. et al., JAP 6, 1954].

This theory proposes that MTT is the ratio between CBV and CBF:

$$MTT = \frac{CBV}{CBF} \tag{22}$$

Combining these two equations 19 and 22:

$$CBF = \frac{CBV}{MTT} = \frac{k_H}{\rho} \frac{\int_0^\infty C_{VOI}(\tau)d\tau}{\int_0^\infty C_{AIF}(\tau)d\tau} \Big/ \int_0^\infty R(\tau)d\tau \tag{23}$$

CBF is the blood flowing in an elementary brain VOI divided by his volume, usually comes in milliliters per 100 grams of tissue per tissue (ml/100g/min) or in microliters per gram per second (µl/g/s).

From equation 23 can be assumed that:

$$\int_0^\infty C_{VOI}(\tau)d\tau = \frac{\rho}{k_H} CBF \int_0^\infty C_{AIF}(\tau)d\tau \int_0^\infty R(\tau)d\tau \tag{24}$$

$$= \frac{\rho}{k_H} CBF \int_0^\infty C_{AIF}(\tau) \otimes R(\tau)d\tau$$

$\otimes$ represents the convolution operator; this operator is justified because AIF is a commutative sum of successive ideal boluses, $C_{AIF}(\tau)\ d\tau$, injected at time τ, so for a time **t** the concentration still present will be proportional to $C_{AIF}(\tau)R(t-\tau)d\tau$ so the concentration will be given by

$$C_{VOI}(t) = \frac{\rho}{k_H}\, CBF \int_0^{\infty} C_{AIF}(\tau)\, R(t-\tau) d\tau$$

If CBF=R' (0)

$$rCBF = \int_0^{\infty} C_{VOI}(\tau) d\tau$$

(25)

Quantification of CBF will be the first step and relies on the deconvolution of equation 25. The second step will be the quantification of CBV from equation 17 and the last step will be the quantification of MTT by equation 22.

3.3. Recirculation, BBB damage and other assumptions.

The dilution theory despite of being considered as true, will not feet completely once the tracer recirculation can happen. Recirculation appears in the results as a second smaller concentration peak, or as an incomplete return to the baseline, meaning that perfusion can only have a good estimation on the first passes of the tracer.

This is due to the fact that Gadolinium do not have a fast elimination, if we take in account that DSC-MRI experiments have the duration of approximately one minute and the gadolinium elimination is mainly done by urinary system and by dispersion phenomena which will take time to allow tracer concentration to get below detection, meaning a lot of time to be processed compared with the time experiment.

So a possible solution is to consider only one passage of the tracer, or in other words consider only the first peak. But the problem will be to separate that peak from the recirculation peak, this can be solved using only the data from the initial peak manifestation to the time that recirculation start or the signal exceeds a certain threshold making it as an arbitrary process. Those are the main problems associated to the recirculation.

Another approach can be done fitting the data to an assumed bolus, for this propose a Gama-variate function is typically used to estimate C_{VOI} data[29][3][31].

$$\mathrm{T}(t; A, \alpha, \beta, t_0) = A.(t - t_0)^{\alpha}.e^{-\frac{t-t_0}{\beta}}$$

(26)

A, α, β and t_0 are parameters that will need to be estimated.

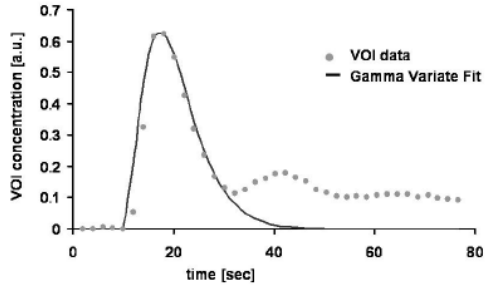

Figure 3.1 Typical concentration time curve of the C_{VOI} with a tracer in the first passage by the VOI (•) and the fitting by Gama-variate function (-) [3]

Another assumption is that BBB is intact, in other words the damage to BBB done by the disease will not be taken in account.

BBB damage result in the escape of the tracer to the extravascular space, this can be a problem because T_1 and T_2* will decrease, making the images whose quality depend on those values worse and introducing a systematic error to DSC-MRI signal.

However, in some diseases, this can be useful if the damage in BBB needs to be found.

A last assumption need to be made, and it is in the conversion of the MR signal to the concentration time curve. This can be a problem because same tissues can have different values due to the vascular morphology and to pulse sequence selected (GE and SE).

GE will have equal weight on venules or arterioles and a smaller value on capillaries, so tissues with different vascularity may have different values in relaxivity.

The same will happen with SE sequence where the signal from tissues with capillaries will be stronger than the same tissues with large vessels.

3.4.AIF measurement

Quantification of CBF, CBV and MTT relies on the knowledge of AIF, so it can be said that AIF is a crucial step.

The correct measurement of AIF is not easy because there is no fixed stereotype which means that is impossible to take into account differences from scan to scan, from patient to patient, from tissue to tissue, from the shape of the bolus injection, from cardiac output, from cerebral vascular resistance and from vascular geometry.

Furthermore $C_{AIF}(t)$ should be extracted as close as possible of the VOI minimizing the dispersion however also mean a value of C_{AIF} for every VOI which is very slow and significant improvements are basically found in patients with ischemia or stenosis ; consequently AIF will be extracted from one the largest vessel that supplies the brain. Meaning that this will be taken as reference for all the brain however this technique will increase the partial volume effect.

For this crucial step some Methods have been proposed.

Direct measurement of AIF is possible via physical blood sampling, however if in one hand this technique gives good values of AIF in the other it is very complex, consuming a lot of time, generating a signal with a weak temporal resolution, making this impractical in clinical imaging [2].

Or directly from DSC-MRI data selecting a small amount of pixels containing one of the principal arterial vessels which can be estimated in two ways manual or by automatic algorithms.

Should be taken in account that DSC-MRI image has low special resolution, the value of a selected vessel can be the result of what is inside the vessel plus some signal generated in the surrounding tissue adding this to the effect of partial volume generated from vessel size, location and orientation, thus an overestimation of CBF is expected.

This second method (direct) is more accepted despite several limitations and errors affecting the measurement. In the manual method will be need a trained operator to select the voxels meaning that the choice will depend on his experience and judgment, so this will be a slow

process with low reproducibility. And in the automatic algorithms many methods have been propose but there is no standard method yet.

Some of those automatic methods are being experimented to correct gaps such as the need of someone with train to select the area where arterial vessel is. Some new methods are based in blind estimation of kinetic Parameters [Jacob U. Fluckiger], use of an appropriate scaling factor [3] or the use of ad hoc correlation methods [3]. Still a lot of work needs to be done. In chapter 4.3 this problem will be discussed again.

In addition to the presence of the effect of partial volume, AIF may suffer dispersion from the point of measurement to more peripheral tissues especially in the presence of pathology. In this case the deconvolved R' (t) represents the CBF multiplied by true residue function (R (t)), and the Dispersion function, d (t):

$$R'(t) = CBF.(R(t) \otimes d(t)) \tag{27}$$

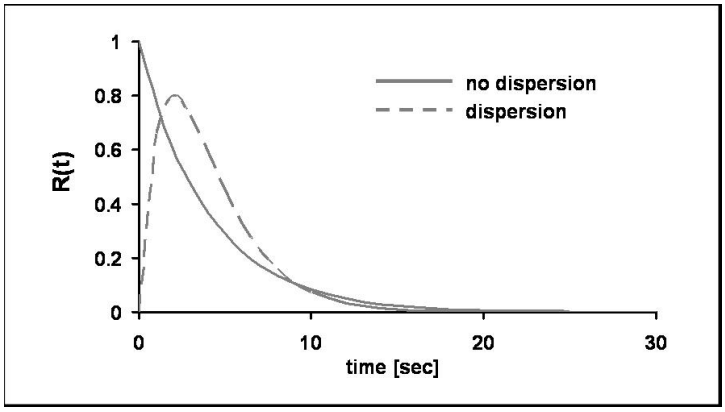

Figure 3.2: Residue Function in absence (solid) or presence (dashed line) of arterial dispersion [29]

CBF is usually estimated from the maximum of the deconvolution curve (figure 3.2 dashed line) where R' (0) =0, $\int_0^\infty d(\tau)d\tau = 1$ and $\int_0^\infty R'(\tau)d\tau = CBF.MTT$, because if

$$R^*(t) = CBF.R(t)$$

Then theoretically $CBF = R^*(0)$ and $R(0) = 1$ (figure 3.2 continuous line); meaning the introduction of a bigger error in CBF quantification.

The type of sequence used can also contribute for C_{AIF} (t) dispersion, however both SE and GE are used because there is no clear evidence that one method will be better than the other in the CBF quantification [32].

3.5.Deconvolution

Deconvolution is exactly what the name suggests it is the process by which the effects of a convolution are reversed, in other words is the reconstruction of the system response from an input signal and the output signal. This process will suffer majorly from two mathematical problems the ill-posedness and the ill-conditioning.

Ill-posedness represents the multiple combinations of the input signal with the system response that can give the same output signal, meaning that with the same input and output signals can be obtained by deconvolution different and equivalent system responses.

Ill-conditioning means that by deconvolution small variations on the output signal (noise) can be amplified introducing a much bigger noise in the system response. Furthermore an acquisition made with a big sampling frequency is not always the best choice because the ill-conditioning increase with the sampling frequency.

There are two main approaches the model-dependent and the model-independent, in this study only model-independent approach will be used. This decision relies on the necessity of a priori assumption on the shape of the solution for the dependent models.

Model-dependent approaches are base in the creation of a parametric function to describe the process losing the ill-posedness and the ill-conditioning, so there are no deconvolution problems anymore but estimation problems which can be solved by shaping the R (t) to a polynomial, to a Gaussian or to a sum of exponentials. But if in one hand has all this advantages in the other deals with the estimation problem, because the solution's shape need to be estimated introducing a big supposition in the Residue function (R (t)).

Model-independent approaches have the advantage of making virtually no assumptions of the unknown functions that will be deconvolved and by this way creates more powerful and less influenced than model-dependent approach, but in this case the deconvolution problems will return.

After those problems another will appear the inverse problem of equation 24.

Fourier transform can be applied because it is known that the transform of two convolved functions is the same as the product of their individual transforms.

$$F\{CBF.R(t) \otimes C_{AIF}(t)\} = F\{C_{VOI}(t)\} \Leftrightarrow$$

$$\Leftrightarrow CBF.R(t) = F^{-1}\left\{\frac{F\{C_{VOI}(t)\}}{F\{C_{AIF}(t)\}}\right\}$$

(28)

F represents the Fourier transform and F^{-1} represents his inverse; the Fourier transform is fairly easy to implement and incentive to delays between AIF and Tissue. This technique is not free from inconvenient, not only it is very sensitive to noise, but also some authors like Ostergaard et al have proved that under some special circumstances (high flow or discontinue residue function) the Fourier transform leads to a unsatisfactory CBF.

In this study Fourier transform will not be used, instead a linear algebraic approach will be used. This method is based in the assumption that tissue and arterial concentrations are measured at equidistant time points so equation 24 can be written has

$$\underset{\substack{Tissue\ Conventration \\ known}}{C_{VOI}(t)} = \underbrace{rCBF}_{\substack{Residue\ Function \\ unkown}} \underbrace{\int_0^t R(t-\tau)}_{\substack{Artirial\ Input\ Function \\ Known}} C_{AIF}(\tau)d\tau$$

(29)

Where r represent relative value because $\frac{\rho}{k_H}$ is assumed as 1.

For a generic time it can be written as

$$C_{VOI}(t_j) = rCBF \int_0^{t_j} C_{AIF}(\tau) \cdot R(t_j - \tau)d\tau$$

(30)

If the data is acquired with a uniform Δt for all the voxels and if the signal cannot change before the arrival of the arterial input.

$$C_{VOI}(t_j) = rCBF \int_0^{t_1} C_{AIF}(\tau) \cdot R(t_j - \tau)d\tau + rCBF \int_{t_1}^{t_2} C_{AIF}(\tau) \cdot R(t_j - \tau)d\tau +$$

$$\ldots + rCBF \int_{t_{j-1}}^{t_j} C_{AIF}(\tau) \cdot R(t_j - \tau) d\tau$$

$$= \sum_{i=1}^{j} rCBF \int_{t_{i-1}}^{t_i} C_{AIF}(\tau) \cdot R(t_j - \tau) d\tau$$

But C_{AIF} is constant, so

$$C_{VOI}(t_j) = \sum_{i=1}^{j} rCBF \cdot C_{AIF}(t_i) \int_{t_{i-1}}^{t_i} R(t_j - \tau) d\tau$$

And

$$t_i = i \cdot \Delta t$$

$$\int_{t_{i-1}}^{t_i} R(t_j - \tau) d\tau = \int_{(i-1)\cdot\Delta t}^{i\cdot\Delta t} R(j \cdot \Delta t - \tau) d\tau, \qquad if \qquad j \cdot \Delta t - \tau = k$$

$$= \int_{(j-i)\cdot\Delta t}^{(j-i+1)\cdot\Delta t} R(k) dk$$

$$C_{VOI}(t_j) = \sum_{i=1}^{j} rCBF \cdot C_{AIF}(t_i) \int_{(j-i)\cdot\Delta t}^{(j-i+1)\cdot\Delta t} R(k) dk$$

(31)

So:

J=1

$$C_{VOI}(t_1) = \sum_{i=1}^{1} rCBF \cdot C_{AIF}(t_1) \int_{0}^{\Delta t} R(k) dk$$

$$C_{VOI}(t_1) = \sum_{i=1}^{1} rCBF \cdot C_{AIF}(t_1) \int_{0}^{\Delta t = t_1} R(k)dk$$
$$= rCBF \cdot \Delta t \cdot C_{AIF}(t_1) \cdot R(t_1)$$

J=2

$$C_{VOI}(t_j) = \sum_{i=1}^{2} rCBF \cdot C_{AIF}(t_i) \int_{(2-i)\cdot\Delta t}^{(2-i+1)\cdot\Delta t} R(k)dk$$

$$= rCBF \cdot C_{AIF}(t_1) \int_{\Delta t}^{2\cdot\Delta t = t_2} R(k)dk + rCBF \cdot C_{AIF}(t_2) \int_{0}^{\Delta t = t_1} R(k)dk$$

$$= rCBF \cdot \Delta t \cdot C_{AIF}(t_1) \cdot R(t_2) + rCBF \cdot \Delta t \cdot C_{AIF}(t_2) \cdot R(t_1)$$

$$C_{VOI}(t_j) \approx CBF \cdot \Delta t \sum_{i=0}^{j} C_{AIF}(t_i) \cdot R\,(t_i - t_i)$$

(32)

And then

$$\begin{pmatrix} C_{VOI}(t_1) \\ C_{VOI}(t_2) \\ \cdots \\ C_{VOI}(t_N) \end{pmatrix} = CBF \cdot \Delta t \cdot \begin{pmatrix} C_{AIF}(t_1) & 0 & \cdots & 0 \\ C_{AIF}(t_2) & C_{AIF}(t_1) & \cdots & 0 \\ \cdots & \cdots & \cdots & \cdots \\ C_{AIF}(t_N) & C_{AIF}(t_{N-1}) & \cdots & C_{AIF}(t_1) \end{pmatrix} \cdot \begin{pmatrix} R(t_1) \\ R(t_2) \\ \cdots \\ R(t_N) \end{pmatrix}$$

$$C_{VOI} = CBF \cdot \Delta t \cdot R \cdot C_{AIF}$$

(33)

This matrix can be simplified to

$$\mathbf{c=A\ .\ b} \tag{34}$$

Where **b** represents the elements of R (t) multiplied by CBF and Δt and **c** represents the tracer concentrations.

$$CBF \cdot \Delta t \cdot R = C_{AIF}^{-1} \cdot C_{VOI} \tag{35}$$

This approach is called the raw deconvolution which is very sensitive to noise, causing R (t) to oscillate.

To overcome some of this problems singular value decomposition (SVD) was introduced in this contest by Ostergaard et al in 1996, where the inverse of C_{AIF} is given by

$$C_{AIF}^{-1} = V.W.U^T \tag{36}$$

Where V and U^T are orthogonal matrixes ($Q^T=Q^{-1}$) and M is a diagonal matrix.

$$CBF \cdot R = \frac{V \cdot M \cdot U^T \cdot C_{VOI}}{\Delta t} \tag{37}$$

This technique reduces the noise on R (t) estimation, this is the result of the elimination of all the values of M which are smaller than a certain threshold. Some studies have been made to establish the best threshold like in reference [7] where the author concludes that the best results are between 15% and 20% of the max value of the diagonal and with this a huge error is erased. Also this technique is sensitive to time delay, some errors remain. It can generate negative values of R (t), which is impossible to have because all the values have to be equal or bigger than zero in physiological cases.

In this paper SVD will be compared with one technique that is immune to time delay and is called Deconvolution Using a Block-Circulant Matrix.

$$C_{VOI} = CBF.A.R$$

Algebraic approach assumes that tissue and arterial are constant between measurements for example in equation (30). Using DSC-MRI in the context of CBF measurements, both Residue Function and Arterial Input Function are expected to diverge over small time scales related with the temporal resolution of the measurements. Consequently cannot be considered that between two consecutive measurements a good approximation is achieved. Consequently is assumed that R (t) and C_{AIF} changes linearly with time and the elements of matrix A become

$$a_{ij} = \begin{cases} \dfrac{\Delta t\left[C_{AIF}(t_{i-j-1}) + 4.C_{AIF}(t_{i-j}) + C_{AIF}(t_{i-j+1})\right]}{6} & if\ \ 0 \le j \le i \\ 0 & otherwise \end{cases}$$

(38)

Using block-circulate SVD deconvolution R' (t) can be represented with R (t) circularly time shift by t_d because AIF can lag C_{VOI} by a delay t_d then $C^*_{AIF}=C_{AIF}$ (t- t_d).
This can be avoided by zero-padding the N values of C_{AIF} and C_{VOI} to length L, where L has double length of N.

Furthermore the elements of matrix A appear as $d_{i,j}=a_{i,j}$ for j<=i and $d_{i,j}=a_{L+i-j,0}$ otherwise. Then equation A can be reformulated after the zero-padding as

$$C = \begin{pmatrix} C_0 & C_{L-1} & \cdots & C_2 & C_1 \\ C_1 & C_0 & & & C_2 \\ \vdots & & \ddots & \vdots & \\ C_{L-2} & & \cdots & C_0 & C_{L-1} \\ C_{L-1} & C_{L-2} & & C_1 & C_0 \end{pmatrix}$$

(39)

After this, the equation (34) can be written as

$$g = C.f$$

(40)

Where d, f and C represent c, b and A after zero-padding. Also using the SVD, the C^{-1} will be

$$C^{-1} = V_c.W_c.U_c^T$$

(41)

Combining with equation (40) f will appear as

$$f = V_c.W_c.(U_c^T.g)$$

In this case a threshold of 10% will be used to eliminate the small values of W because *Ostergaard et all* in is his work propose that the best results for this technique came with this value

4. Methods

4.1.Clinical data

Clinical data includes ten relapsing-remitting (RRMS) patients with median EDSS 2.0 (7 women, 3 men; age range 19-45 years) were consecutively enrolled in this study. The diagnosis was based on agreements with the International Criteria (McDonald et al, 2001; Polman et al, 2005). Informed consent was obtained from all patients and the study was approved by the local Ethic Committee.

MRI acquisition was performed on a 1.5-T Philips Achieva scanner (Philips Medical Systems, Best, Netherlands).

Figure 4.1Philips Achieva 1.5T [40]

Not every analysis done by the machine will be used; in this case for example 3 analyses will be done:

- 3-dimensional fast field echo, 3-dimensional sequence with 120 contiguous axial sections with the off-center positioned on zero (TR=25 ms; TE=4.6 ms; flip angle=30°; section thickness=1.2 mm; FOV=250x250 mm^2; matrix=256x256);

- Double Inversion Recovery (DIR): 2-dimensional multisection sequences with 50 contiguous axial sections (TR=15631 ms; TI1=325 ms; TI2=3400 ms; section thickness=3 mm; FOV=250x250 mm2; matrix=256x256; gap between slices=0 mm);

- Dynamic Susceptibility Contrast MRI (DSC-MRI): 120 T2*-weighted volumes were acquired before and after the injection of bolus of gadolinium Gd-DTPA (bolus dose=0.1 mg/kg; sequence settings: TR=1375 ms; TE=40 ms; flip angle=90°; section thickness=6.0 mm; FOV=230x230 mm2; matrix size=256x256; gap between slices=1 mm; 120 total volumes);

4.2.Extraction and mask

4.2.1. Signal acquisition

DSC-MRI has as main goal the reading of the MR during the passage of the tracer on the VOI which will attenuate the signal, with it discover the C_{VOI} and after that all the hemodynamic parameters (CBF, CBV and MTT). During this phase the best of the machine will try to be achieved and in this case we talk about a small repetition time, a signal with low noise and with good quality and a high spatial resolution.

However it will be impossible because if any of those points is improved some other will get worse as seen before. So a good relation between them has to be achieved and for that a protocol has to be established.

For TR, the acquisition must not be bigger than 2 seconds because if the TR is to big the tracer progress curve will not be well represented especially in the main peak, so a small TR is required.

With this equipment DSC-MRI will give a low resolution normally it will be 128 by 128 pixels, compared with other equipment that can reach 1024 by 1024 pixels per image. This parameter will establish the voxel dimension. For example if a Field of view (FOV) of 200mm is used the voxel dimension will be 200/128 which is approximately 1.6 X 1.6 mm. So can be said that a machine with a better resolution will improve the partial volume effect and the anatomic detail.

The tracer sensibility in particular T_1, T_2 and T^*_2, are influenced and modulated by the TE which must be maintained between 40 and 50 ms to secure a FID with a good amplitude and by the Flip angle, in this case will be used at 90^0 to maximize the T^*_2 value [29].

4.2.2. Data extraction

All the data analyze done in this work have been done in MatLab (Matrix Laboratory) version 7.11.0.584 (R2010b) product of MathWorks, Inc. c 1984-2010.

MatLab software by itself is not enough to convert the signal, so for this propose another MatLab application is needed: *NIfTI Toolbox*, this is free software and is available at

`http://www.rotman-baycrest.on.ca/~jimmy/NIFTI/`

4.2.3. Mask

MRI data need to be treated meaning that all the parts that are not brain have to be filtered, this means that all the values under threshold will be eliminated from the data. Thus, a threshold value will be generated by analyzing the data and his distribution.

This distribution can be represented in an intensity histogram where can be realized that the distribution of the signal represents the junction of two kinds of signal, meaning that one of them represents the signal inside the brain and the other represents some noise inside the image (outside the brain, measuring errors and non-physiologic values).

Many thresholds can be chosen; manually choosing one or two values of the image if two points are chosen, one will be at the beginning and another at the end, eliminating the biggest and the smallest values that may not be physiological.

It can even be chosen a point related to the fit interception of the tow signals present in the histogram. If it is chosen a point before the interception more points of interest will be added but will happen the same with the noisy points, the opposite happened if we chose a point in the other side of the interception.

However in this study will be fixed a threshold of minimal error, meaning that the interception of the both curves will be chosen.

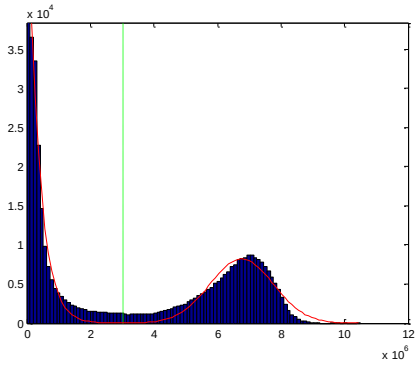

Figure 4.2 The blue bars represent the concentration distribution and the green line represents the threshold of minimal error

The mask obtained will have a well-defined border but it is no guaranteed that all the values inside are on it so all the values surrounded through all sides by the mask will be added to the accepted values. All groups of values smaller than two hundred pixels will not be accepted so possible pieces of the scalp will be removed.

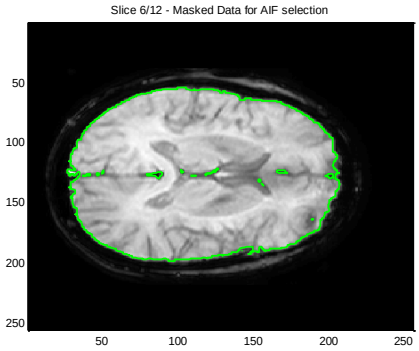

Figure 4.3 Mask with discontinuities

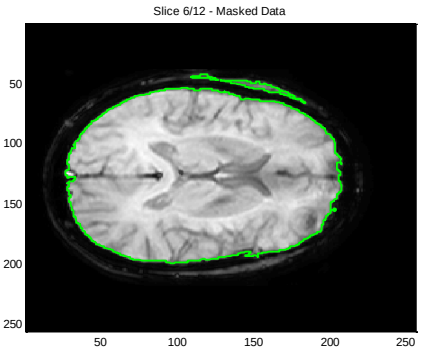

Figure 4.4 Mask with values outside the brain

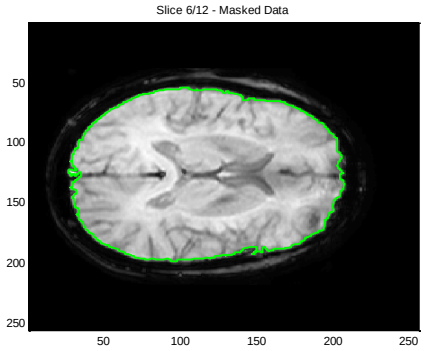

Figure 4.5 Final ask selection

In figures 4.3, 4.4 and 4.5 is the image of the slice 6 of a brain and the green line represents the boundaries of the selected values.

4.3.C_{VOI} and S_0 map

S_0 value will be created from the mean of the firsts values, the choice of this values will depended on a thresholds in this case

$$S_0 = \left|\frac{mean(a) - mean(a+1)}{mean(a)}\right| < 0.05 \quad \textbf{(42)}$$

Where *a-1* represents the firsts values that satisfy the equation.

This value will be used to calculate the S_0 map because this will be generated by the values until t=a-1.

$$S_0 map = mask \cdot MRI\ signal(0: a-1) \quad \textbf{(43)}$$

S (t) will result from the mean of the signal of the slice for the time t.

C_{VOI} will be generated from equation 12 (all the values bigger than S_0 will take the value of S_0).

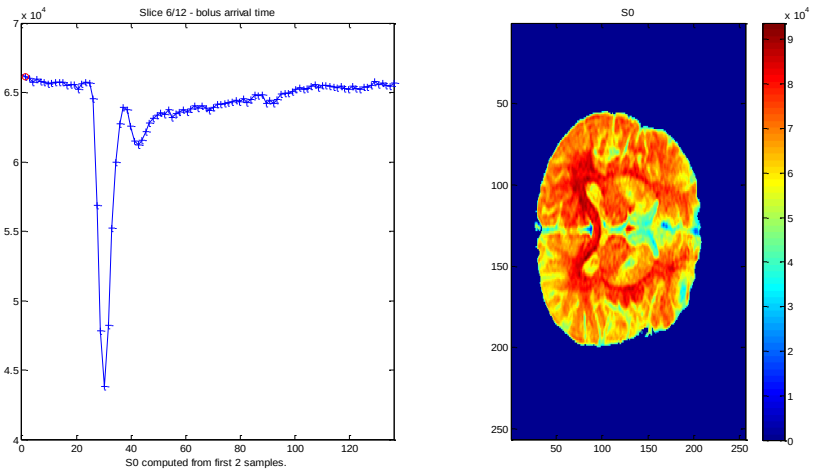

Figure 4.6 Tissue signal on the left and S_0 on the right

4.4.AIF

AIF is a crucial step. Among the methods published, only those which present an automatic selection have interest in this paper. The method proposed by K. Mouridsen et al (2006) and the one proposed by A. Rempp et al (1994) are two good examples.

In this paper a new method proposed by D. Peruzzo et al [32] will be used. This method can be summarized in few steps:

The first step is too chose a slice of the brain. This slice must contain the region where the main central artery (MCA) is present in order to minimize the delay in the AIF. A slice from the middle upper part of the brain will provide good results, not only because the lesions of the MS will majorly be there, but also the lower slices will contain noise produced by the undesirable tissues.

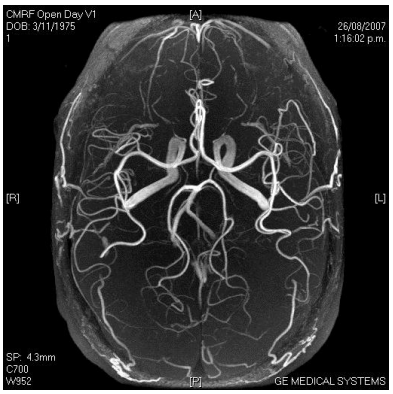

Figure 4.7 Blood brain vessels [33]

The selected region (ROI) will be an ellipse centered between the first and last voxel taken in account as brain; fig.4.7, this will get almost the central area of the brain and consequently the area where MCA main segment is supposed to be fig.4.6.

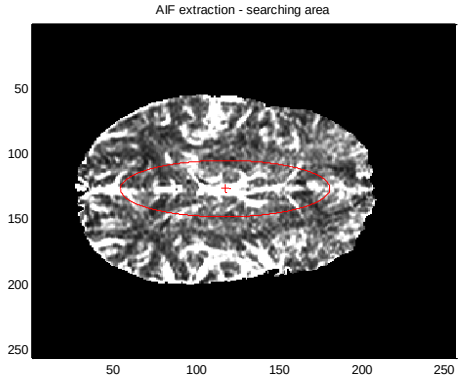

Figure 4.8 Region where AIF will be estimated

Secondly the voxels inside the VOI have to be filtered starting with the elimination of all those which stay under a certain limit in this case three filters were used.

First filter is based on the elimination of the voxels with smaller area under curve (AUC), in other words this means that AUF is the integral of every voxel. This will allow the minimization of the partial volume. The amount of elimination will depend on the programmer but in this case 40% will be eliminated [D. Peruzzo, et al].

Second filter is based in the time to peak (TTP) elimination. All the voxels with a delayed TTP will be eliminated. These voxels are associated to large venous structures (veins and venules). The amount of elimination will depend on the programmer. In this case will be eliminated 40% [D. Peruzzo, et al].

Third filter is the irregularity filter which leads to the elimination of ate least 0.05% [D. Peruzzo, et al] of the more irregular values.

The irregularity index is given by

$$I_{reg} = \int_0^{\infty} \left(\frac{\partial^2 C(t)}{\partial t^2} \right)^2 dt \qquad \textbf{(44)}$$

Finally a cluster analysis will be implemented to extract the voxels with arterial values; this method will combine the two nearest voxels or clusters using Euclidean distance. This will be repeated until all the voxels are in two final big groups, the goal of this part is to maximize inter cluster variation and minimize intra cluster variation.

Then the cluster with the highest centroid peak (mean cluster curve) is selected, but if the difference between the two means is smaller than 5% the selection method will change and the selected cluster will be the one with smaller time to peak. This process will be repeated in the selected cluster until it encloses only six or less voxels.

AIF will be estimated from the mean of the selected voxels.

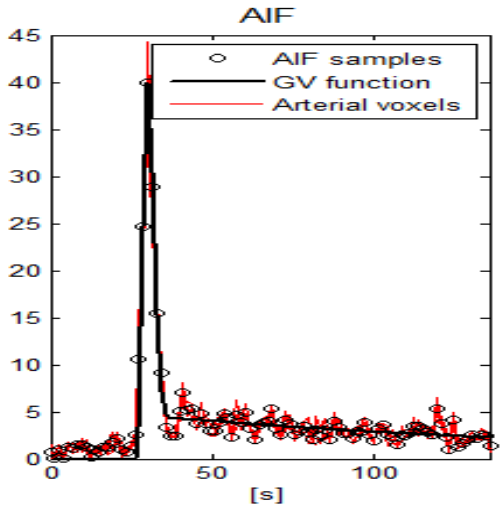

Figure 4.9 AIF distribution

4.5.Gray matter Mask and lesion Mask

Gray matter was separated from all the other brain matter by an operation of segmentation with a statistic basis. This data was provided by Marco Castellaro, and it was a probability map where the probability of a certain tissue to be gray matter for all patients and for all slices was represented.

In this case only voxels with a probability of 90% or more where chosen as gray matter, and with this threshold can be assured that almost of the voxels are from gray matter.

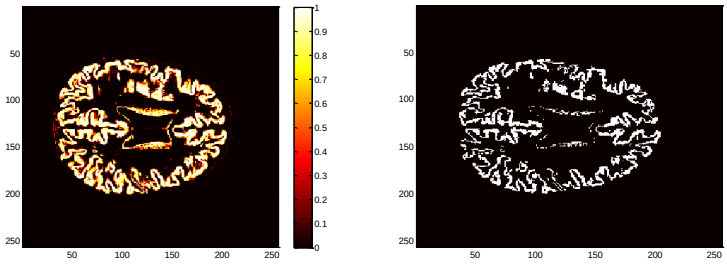

Figure 4.10 in the left is the probability map of being gray matter, in the right is the image with all the voxels over a threshold of 90% (this data was extracted from patient 1 slice 8)

All the lesions where selected manually by a neurologist with experience on this field.

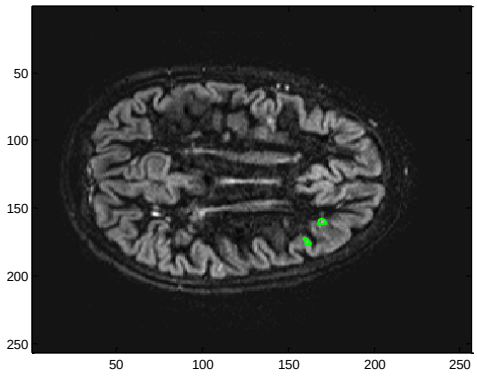

Figure 4.11 GM lesions appear as green in the figure; this data was extracted from patient 1 slice 8

4.6.CBV, CBF and MTT

CBV was extracted by formula (17) taking the constants as one.

CBF was extracted base on the deconvolution of AIF with C_{VOI} and from two different processes SVD and cSVD.

The process can be reversed by convolution if the residue function (R (t)) is stored.

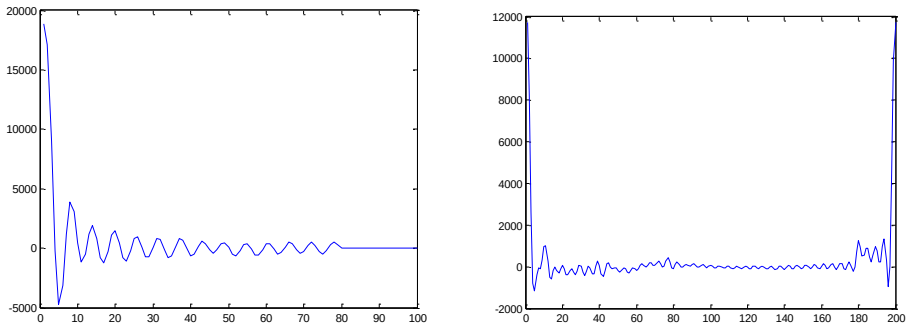

Figure 4.12 singular value decomposition R (t) on the right and cSVD R (t) on the left; both for a random point

MTT will be generated by function (22). In the end there will be a map for every parameter with SVD and cSVD, figure (4.13).

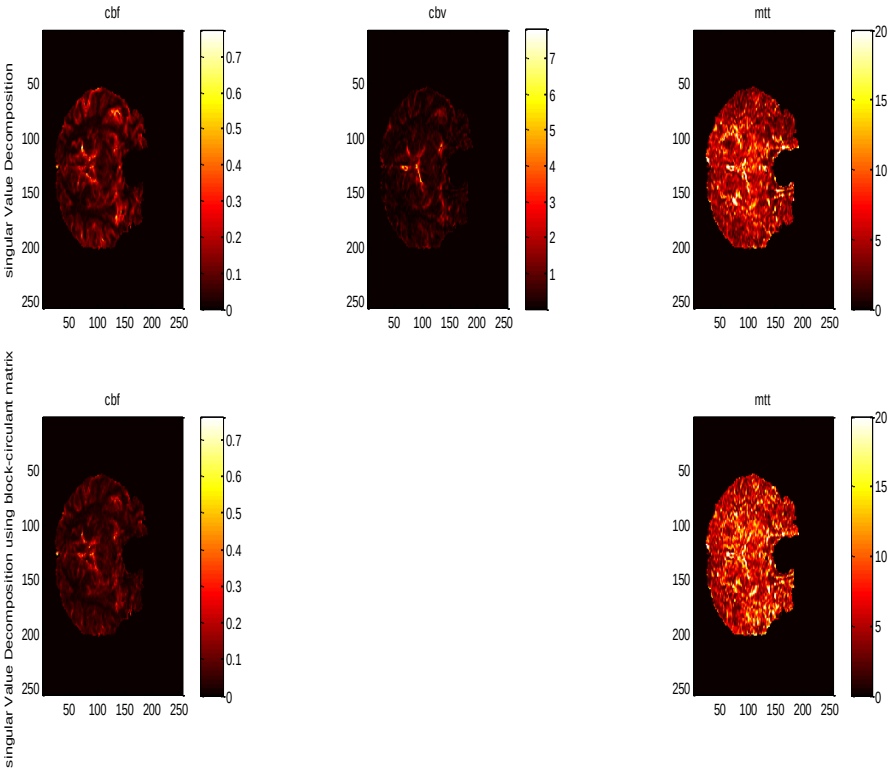

Figure 4.13 images for SVD and cSVD in CBF and MTT, CBV will be equal for both.

CBV and CBF will be truly dependent on the brain density (ρ), H_{LV}, K_{VOI} and H_{SV}, basically all the values are taken as constants, but in reality they will change from patient to patient and from machine to machine. Due to this CBV and CBF have all the constants taken with no value (=1).

These mean that only relative values of CBF and CBV can be obtained. To overcome this problem will be study the rate percentage between the normal appearing gray matter (NAGM) and the lesion in the gray matter.

For this propose the mean of all parameters (CBF, CBV and MTT) will be calculated for the NAGM in the hole slice and for each Lesion and for every lesion will be applied the equation

$$Relation = \frac{NAGM - Lesion}{NAGM} \tag{45}$$

In the end all the results will not have dimension. However the characterize of hemodynamics from the gray matter will be possible.

4.7.Overview of the methods

1. Use the *NIfTI Toolbox* to extract DSC data to a format that matlab can read.
2. Selection of the tissue of interest applying the mask present in chapter 4.2.3 to the extracted data.
3. S_0 will be calculated from the values that did not present an intensification over a certain threshold.
4. C_{VOI} will be calculated from equation (12)
5. AIF will be extracted as present in the chapter 4.4
6. CBF will be extracted by SVD and cSVD and then compared
7. CBV and MTT will be extracted from equations 17 and 22 respectively and then calculated for SVD and CSVD
8. The masks from gray matter and from lesions will be made
9. CBF, CBV and MTT will be extracted for gray matter and gray matter lesion multiplying the maps from point 6 with the respective mask.
10. The mean of all maps from point 9 are estimated and the function (45) applied
11. The results from all the lesions of all patients are compiled and then the Mean and the standard deviation are estimated
12. A t test will be applied in the results

5. Results

This study has as main goal the analysis of brain hemodynamics and for that some parameters like CBV, CBF and MTT will be studied in every patient. Furthermore this parameter will be studied by two different processes SVD and cSVD.

The relation between SVD and cSVD can be studied by visualizing their pseudo concentration and the convolution of the R (t) and AIF (figure 5.1)

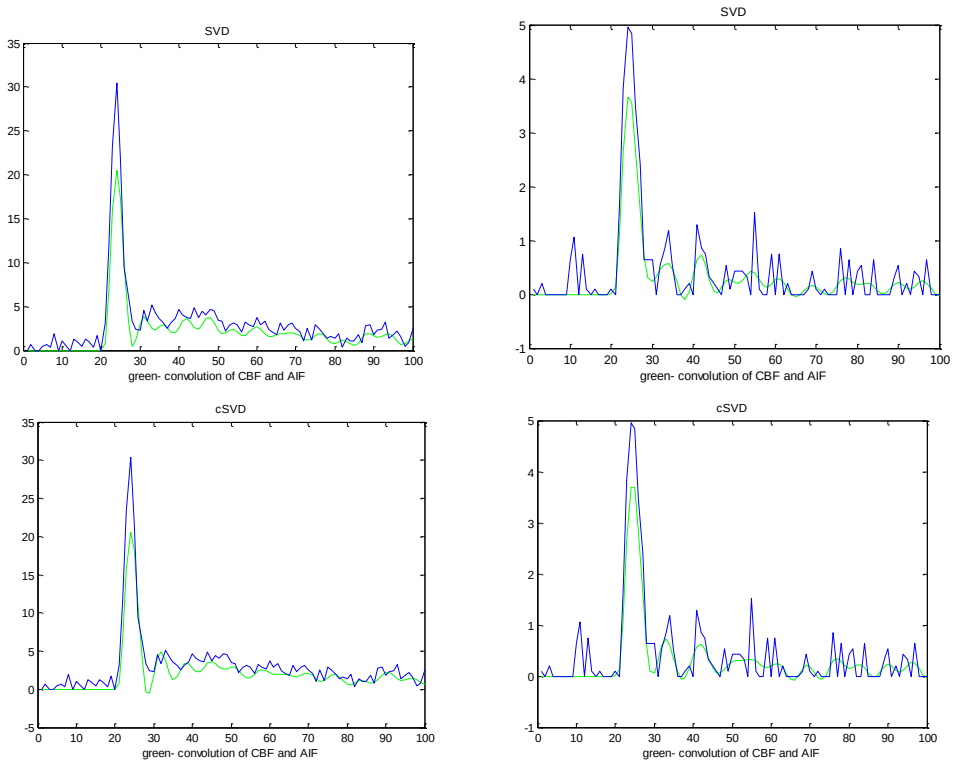

Figure 5.1 representation of the concentration of two points, in blue will be the pseudo concentration and in green is the concentration given by the convolution of CBF and AIF. The right side represents one point and the left side represents another. The top graphics where realized with SVD and the bottom ones where realized with cSVD.

With these results, it can be said that cSVD gives a slightly better approach. However both approaches will be studied and in the end the results will be compared to understand if the differences are significant.

It can also be seen that signals in the convolution have the first part constant, this is due to the fact that the tracer has not arrive yet. After this point there is a rapid increase on the value

(main peak), the signal also present, next to the peak, a parte with some oscillation that can be explained by recirculation of the tracer.

With the decision of studying both SVD and cSDV, the CBF, CBV and MTT were obtained in both. These values were separated in NAGM and gray matter lesion and the mean was calculated.

After this where discover that with the gray matter at 90% patient 7 has no lesions in the gray matter and patient 10 have lesions but they are to small (<5 voxels), meaning that this patient cannot be used.

This elimination is necessary because in small legions the statistics is very influenced by every voxel, meaning that one voxel with undesired or non-physiological values can ruin the mean value.

Table 5.1 Number of pixels selected in patient 10 as lesion with a threshold of 90% for the probability of gray matter

lesion	number of pixels
12	2
12	3
12	3

Then the mean of CBF, CBV and MTT from NAGM and from all the lesions where extracted. For example the results from the third patient can be found in fig (5.4, 5.5 and 5.6)

CBV is not affected by SVD or CSVD because it is measured before the deconvolution.

During this procedure were added two thresholds which will turn all the negative values and all the values bigger than 150 equal to zero, in other words the voxels with non-physiological values where removed.

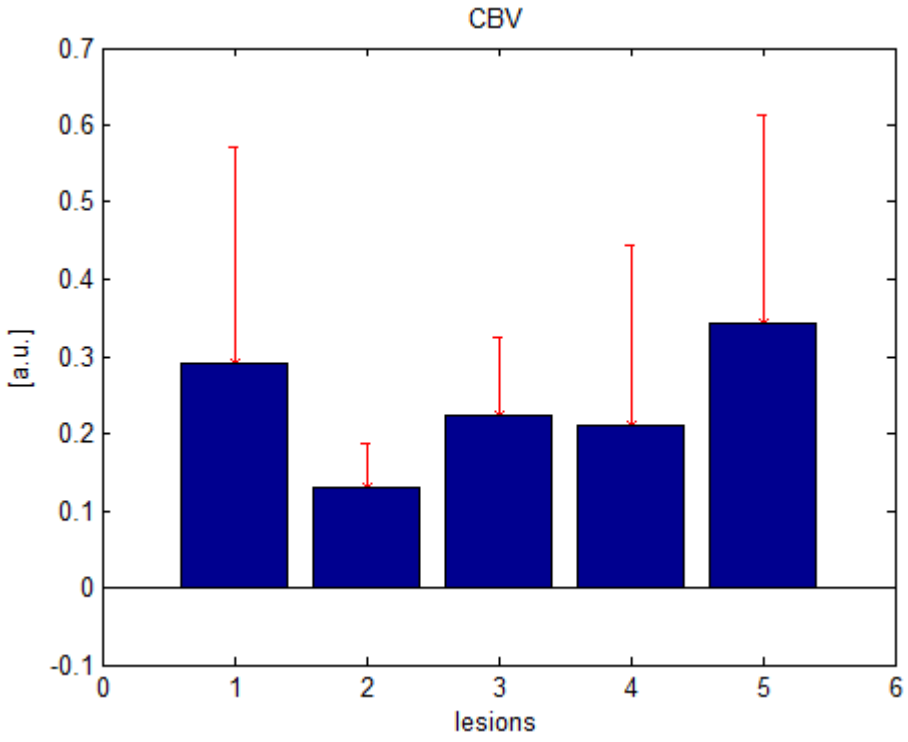

Figure 5.2 CBV mean and SVD for all the lesions bigger than 5 voxels in patient 3, the first bar represents the mean of CBV in NAGM

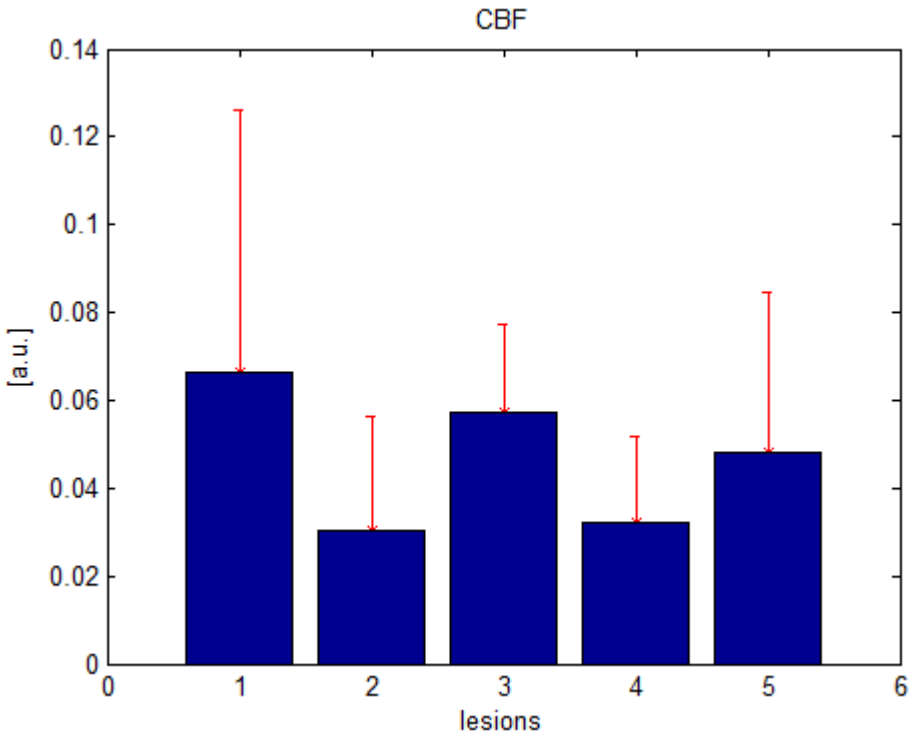

Figure 5.3 CBF mean and SVD for all the lesions bigger than 5 voxels in patient 3, the first bar represents the mean of CBF in NAGM

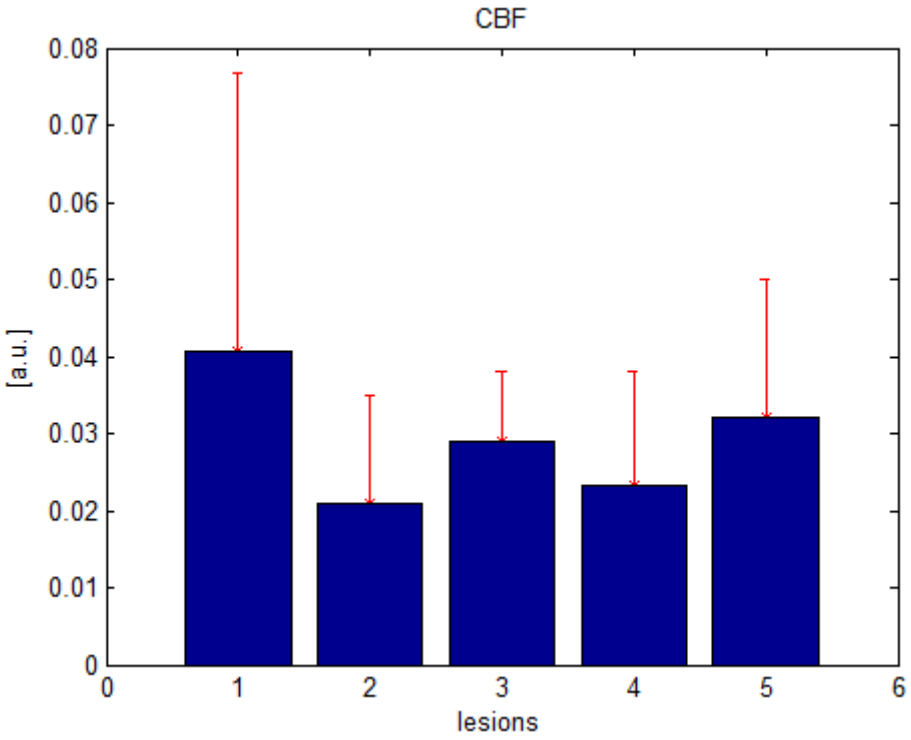

Figure 5.4 CBF mean and cSVD for all the lesions bigger than 5 voxels in patient 3, the first bar represents the mean of CBF in NAGM

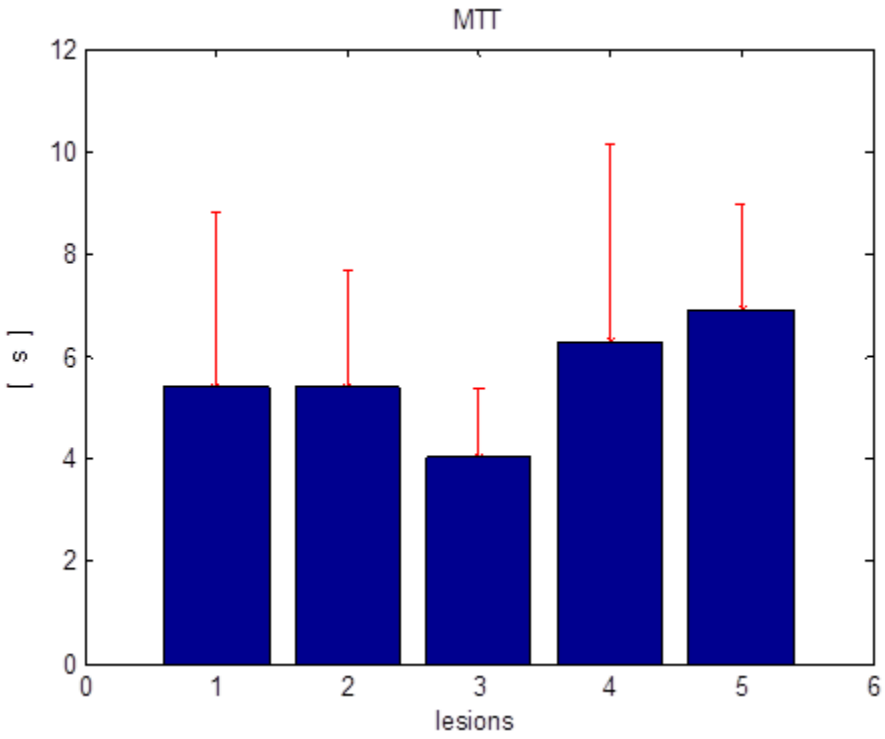

Figure 5.5 MTT mean and SVD for all the lesions bigger than 5 voxels in patient 3, the first bar represents the mean of MTT in NAGM

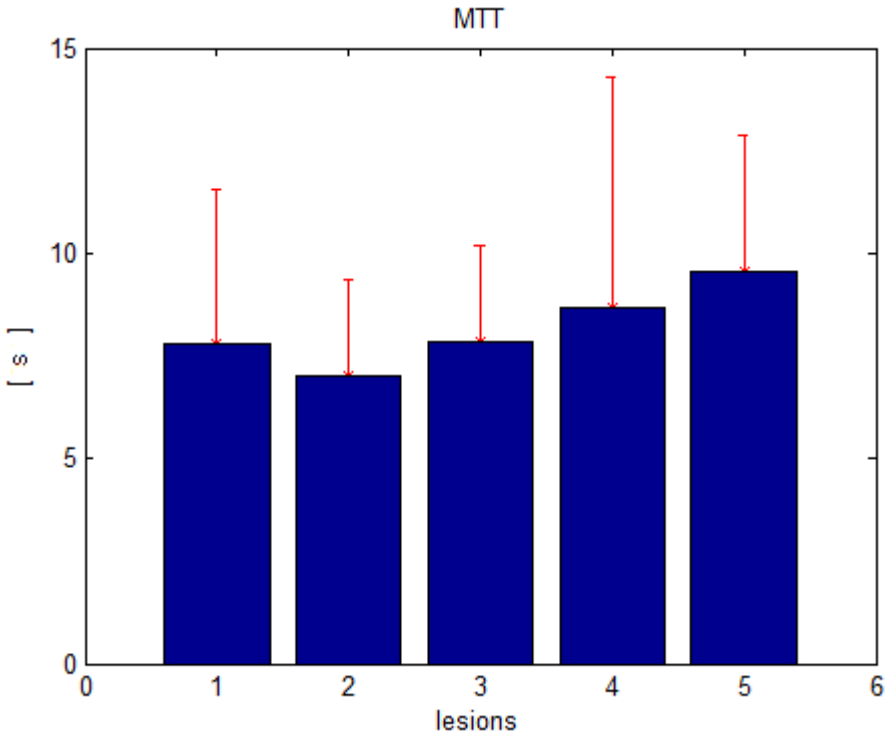

Figure 5.6 MTT mean and cSVD for all the lesions bigger than 5 voxels in patient 3, the first bar represents the mean of MTT in NAGM

Figures 5.2, 5.3, 5.4, 5.5 and 5.6 represent the mean of hemodynamic parameters of patient 3. The first column represents the mean of NAGM, and the next four columns represent the four lesions present in patient 3.

From the CBF and CBV, there is nothing significant to conclude since these values are relative values and cannot be compared in other subjects. Still it is possible to compare it inside the same subject.

It is known that all the lesions where selected by an experienced doctor and is also known that the fist bar of all the graphics from figure 5.2 to 5.6 is not a lesion but the mean of the NAGM.

This tells us that all those values after the first have to be from lesions. Then a CBF or a CBV from a lesion smaller than NAGM represents an old lesion where the tissue damage leads to a decrease of the local metabolism, and as consequence, a decrease of the perfusion (CBF). However if the CBF or CBV is smaller it can represent a lesion at the first inflammatory phase.

MTT in not a relative value because it results from the division of the CBV and CBF and the unknown constants are divided by theme selves. This will give the possibility to study MTT in this step; MTT will be in seconds.

However MTT will have no important meaning, because as shown further ahead, there is no statistical difference between subjects (P value bigger than 0.05 in table 5.4 for MTT).

To study this theory and to allow CBF and CBV to be studied, the percentage difference (equation (45)) between NAGM where the lesion was found and the MS lesion were analyzed. For that, firstly it will be presented the patient number three and afterwards it will be presented the data from all the patients. All the subjects' data had the same treatment; patient number three was randomly chosen as example.

Patient number 3

Table 5.2 Representation of the relation between NAGM and lesions for CBV, CBF and MTT and the respective mean, standard deviation and p value (p value is extracted from a t-test with a significance of 0.05) for patient 3 using SVD

lesion	CBV	CBF	MTT	number of pixels
10	0,215	0,143	0,247	43
10	0,544	0,543	-0,003	45
11	0,235	0,436	0,003	18
11	-0,250	0,153	-0,093	33
mean	0,186	0,319	0,038	
p value	0,338	0,051	0,634	

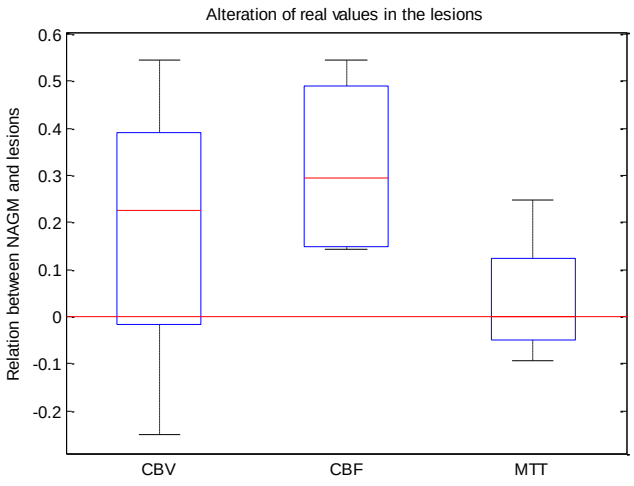

Figure 5.7 Dispersion of the relation between NAGM and lesions for all the Hemodynamic parameters in patient 3 using SVD

Table 5.3 Representation of the relation between NAGM and lesions for CBV, CBF and MTT and the respective mean, standard deviation and p value (p value is extracted from a t-test with a significance of 0.05) for patient 3 using cSVD.

lesion	CBV	CBF	MTT	number of pixels
10	0,215	0,199	0,076	43
10	0,544	0,422	0,169	45
11	0,235	0,349	0,0002	18
11	-0,250	0,103	-0,102	33
mean	0,186	0,268	0,036	
p value	0,338	0,034	0,578	

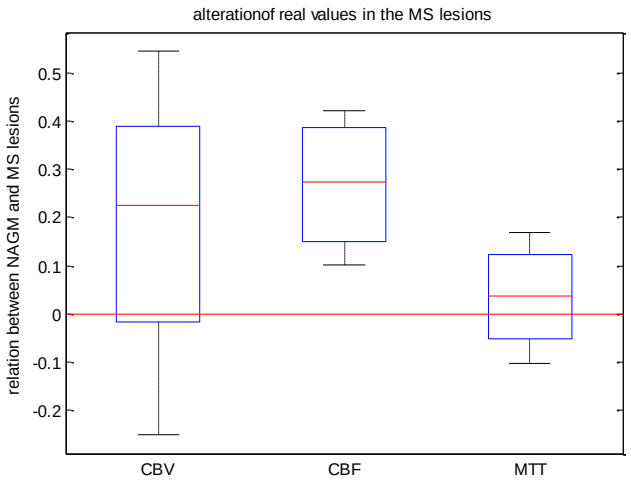

Figure 5.8 Dispersion of the relation between NAGM and lesions for all the Hemodynamic parameters in patient 3 using cSVD

All patients

Table 5.4 Representation of the relation between NAGM and lesions for CBV, CBF and MTT and the respective mean, standard deviation and p value (p value is extracted from a t-test with a significance of 0.05) for all patients with lesions with at least 5 pixels per lesion; in the left side all the parameters are obtained with SVD and in the right side it was used cSVD.

patient	CBV	CBF	MTT
1	-0,167	-0,730	0,343
	0,204	0,149	0,069
	0,779	0,687	0,335

CBV	CBF	MTT
-0,167	-0,442	0,193
0,204	0,155	0,033
0,779	0,679	0,333

	0,522	0,635	-0,226	0,522	0,659	-0,356
	0,124	-0,490	0,433	0,124	-0,224	0,286
	0,249	-0,054	0,226	0,249	-0,010	0,241
	-0,120	-0,087	-0,404	-0,120	-0,059	-0,223
	-0,166	0,062	0,019	-0,166	0,052	-0,225
	0,439	0,587	-0,284	0,439	0,529	-0,121
	0,676	0,668	0,032	0,676	0,566	0,278
	-0,352	-0,350	0,107	-0,352	-0,047	-0,208
	-0,013	0,167	-0,151	-0,013	0,205	-0,195
	0,586	0,753	-1,222	0,586	0,664	-0,234
2	0,167	-0,317	0,369	0,167	-0,145	0,292
	0,006	0,388	-0,409	0,006	0,394	-0,646
	-0,018	-0,290	0,330	-0,018	-0,117	0,165
3	0,215	0,143	0,247	0,215	0,199	0,076
	0,544	0,543	-0,003	0,544	0,422	0,169
	0,235	0,436	0,003	0,235	0,349	0,0002
	-0,250	0,153	-0,093	-0,250	0,103	-0,102
4	-0,595	-0,357	-0,161	-0,595	-0,381	-0,162
	0,064	-0,112	0,281	0,064	-0,035	0,133
5	-0,944	-0,069	-0,703	-0,944	0,021	-0,842
	0,375	0,192	0,203	0,375	0,209	0,159
	0,120	0,135	-0,046	0,120	0,057	0,029
	0,023	-0,022	0,321	0,023	0,002	0,288
	0,120	0,162	0,045	0,120	0,136	0,069
	0,471	0,497	-0,067	0,471	0,505	-0,106
	-1,018	-0,521	-0,254	-1,018	-0,442	-0,332

	0,385	0,656	-0,967	0,385	0,741	-1,683
	0,444	0,327	0,181	0,444	0,261	0,262
	0,536	0,505	0,031	0,536	0,493	0,044
6	0,581	0,523	0,288	0,581	0,548	0,157
	0,501	0,501	0,125	0,501	0,509	0,071
	-0,280	-0,349	0,251	-0,280	-0,290	0,145
	0,599	0,537	0,103	0,599	0,541	0,105
	0,603	0,395	0,413	0,603	0,437	0,319
	0,642	0,632	0,008	0,642	0,601	0,112
8	0,643	0,595	0,184	0,643	0,548	0,195
	0,350	-0,005	0,371	0,350	0,054	0,327
	0,328	0,376	-0,089	0,328	0,365	-0,063
	0,432	0,670	-0,335	0,432	0,686	-0,416
	0,152	-0,769	0,530	0,152	-0,471	0,412
	0,502	-0,091	0,582	0,502	0,155	0,430
	0,559	0,709	-0,606	0,559	0,739	-0,752
	0,669	0,807	-0,643	0,669	0,698	-0,072
	-0,521	-0,069	-0,280	-0,521	-0,045	-0,287
	-0,066	-0,189	0,158	-0,066	-0,262	0,186
	0,322	0,214	0,159	0,322	0,307	0,048
9	-0,376	-0,497	0,141	-0,376	-0,376	-0,465
	0,317	0,111	0,305	0,317	0,202	0,235
mean	0,188	0,168	0,005	0,188	0,205	-0,033
SD	0,411	0,417	0,370	0,411	0,370	0,373
P	0,002	0,006	0,925	0,002	0,002	0,526

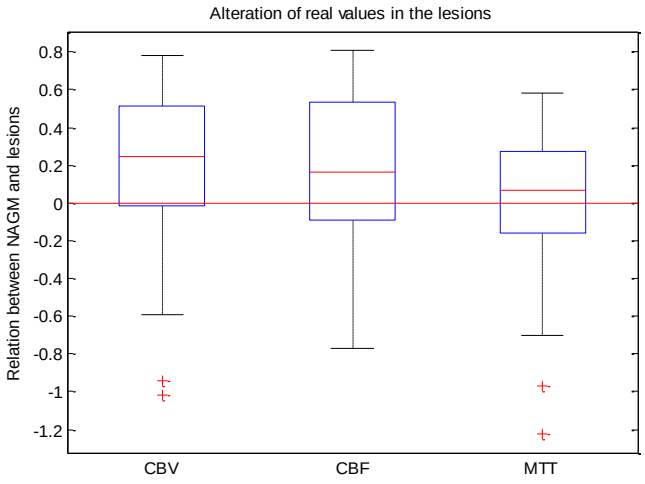

Figure 5.9 Dispersion of the relation between NAGM and lesions for all the Hemodynamic parameters in all the patients using SVD

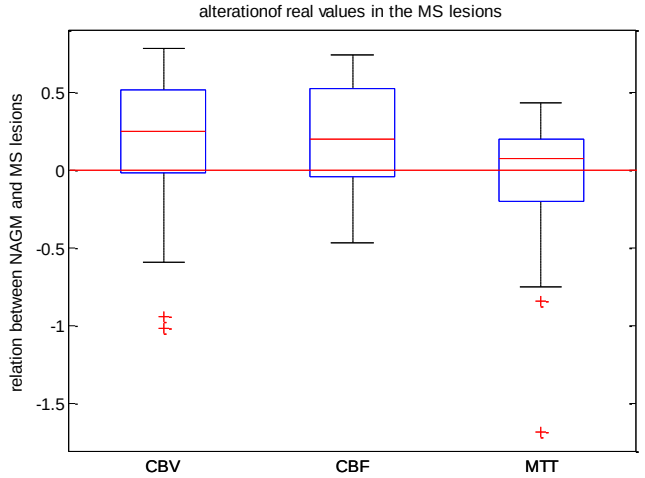

Figure 5.10 Dispersion of the relation between NAGM and lesions for all the Hemodynamic parameters in all the patients using cSVD

The relation between NAGM and lesion for all lesions of patient 3 in terms of hemodynamic parameters (CBV, CBF and MTT) using SVD is represented in table 5.2. Table 5.3 is represents basically the same thing as figure 5.2, but in this case using cSVD; the last three lines of each table represent the mean, the standard deviation and the p value respectively. It can be seen from the mean that CBV and CBF have lower values compared with NAGM, however MTT will have minimal oscillations.

In table 5.4 a global perspective is obtained on the left for SVD and on the right for cSVD. This table is stratified in the same way as the two previous tables. Even the results are similar once MTT values have only small changes and CBF and CBV have smaller values than NAGM meaning that subject three is a good reference.

In all those tables, the last line is the p value which is obtained by the t-test, in this study the used a significance is $\alpha=0.05$.

Figures 5.7, 5.8, 5.9 and 5.10 allow an easy visualization of the data distribution (all the parameters are represented in the box-plot) where it can be verified that there is a tendency for CBF and CBV to get smaller results in the lesion in comparison with the NAGM, and the MTT to stay in the same values, meaning that in our data there are more lesions where the level of tissue damage has already lead to a decrease of the local metabolism, in other words not the lesions in earlier stages which are represented by the red "+" and by the dashed line on the lower part of all the boxplots.

Furthermore the p value will only reinforce the idea that there are significant statistical differences between the hemodynamic values (CBF and CBV) in the lesion and in the NAGN, because for those two the p value will be lower than 0.05, meaning that they are not related to a distribution around zero. This did not happen to MTT that has big p values, which means that there is no statistical difference between MTT in the lesion and in the NAGM.

6. Discussion and conclusion

In this study it was established that the two main deconvolution methods, SVD and cSVD will be tested and compared.

There was only one test performed to compare those technics in terms of the deconvolution process and it is presented in figure 5.1. To obtain these results, the convolution of R (t) with AIF was made in order to reach a pseudo concentration which can be compared with C_{VOI}.

This technic is not totally reliable because it will depend on the person who analyses it and in the voxel chosen for the experiment, because different voxels have different noise. However in this case was establish that the results from the cSVD were better because the SVD results may carry an under estimation of the concentration.

If SVD and cSVD need to be compared, other technics have to be applied.

In the next step, the small lesions (<5) were discarded because, if in one hand they are actually lesions and statically with more data better results can be obtained, in the other hand all lesions will have the same weight, meaning that if a pixel in a small lesion has a bad value it will introduce a big error. Furthermore in legions that are too small, some statistical processes cannot be applied.

After this there is another problem, which will have its base in the differences between every person in terms of the vessel structure inside the brain, blood input or brain density. This will lead to the elimination of constants, i.e., the constants will be taken as 1.

Still it can be done but with some costs because all the values created by this way will be relative values (figures 5.2, 5.3 and 5.4), meaning that all the values are dependent on some constants that will diverge from patient to patient.

To solve this problem, the values will not be compared directly between patients, but instead by using the percentage between the difference on GM lesion and NAGM, and by this way it will be possible to eliminate the unknown constants from the equation allowing the hemodynamic parameters to be compared in different subjects.

In the end, there was no significant difference between the results obtained by SVD and cSVD, despite of the results from cSVD being less spread than the results from SVD.

It can be said that the results from this experiment were satisfactory regarding the hemodynamic in the multiple sclerosis with DSC-MRI.

7. Future considerations

After this start, where the program was tested, many more studies can be done to understand the disease in all of its variants.

For this propose many more persons with the disease need to be taken in account and in this point of view not only persons from one place, because is known that this disease has different incidence rates depending on many factor. Thus a relation or a divergence could be found.

Furthermore the disease could also be studied in the other parts of the brain not only in the gray matter and the same patient could be studied over time allowing a better understand of the disease development.

Or the SDC-MRI could be combined with other technics that are being develop like Susceptibility weighted imaging (SWI) or Arterial Spin Labeling (ASL)

7.1. Susceptibility weighted imaging (SWI)

Until recently, MRI was only dependent on the magnitude of information and tissue phase was rejected or even discarded before getting to the viewing console, however phase images can be very important and used in MR applications.

Phase images are only possible because some tissues have magnetic susceptibilities considerably different from background and surrounding tissues. Some examples are deoxygenated blood, hemosiderin, ferritin, clots, calcium, iron-laden tissue or air/tissue.

Meaning that many diseases that can get lots of advantages, such as neurodegenerative disorders, stroke, trauma, vascular malformations, neurocysticercosis, tumors and TBI: diffuse axonal injury [19][18][17].

This technique was discovered some time ago but was not used for almost 20 years because of the presence of a magnetic background field that confounded the suitable phase information.

After 1997, E. M. Haacke et all [18] create a method to remove most of unwanted background and artifacts keeping the suitable phase information. This was the breakthrough allowing this method to be used and the really applications to be discovered.

After this, phase images were possible and with it an excellent source of contrast information allowing, among other things, the creation of a phase mask to work by itself, creating images to study tissue contiguity, to suppress/enhance spectral components or study contrast modifications.

This last information can be combined with magnitude images altering his contrast. This method receive the name of Susceptibility weighted imaging (SWI) [17][18].

For this technique to be used firstly a high pass (HP) filter needs to be apply removing low spatial components; for example imperfect shim or cavities field with air.

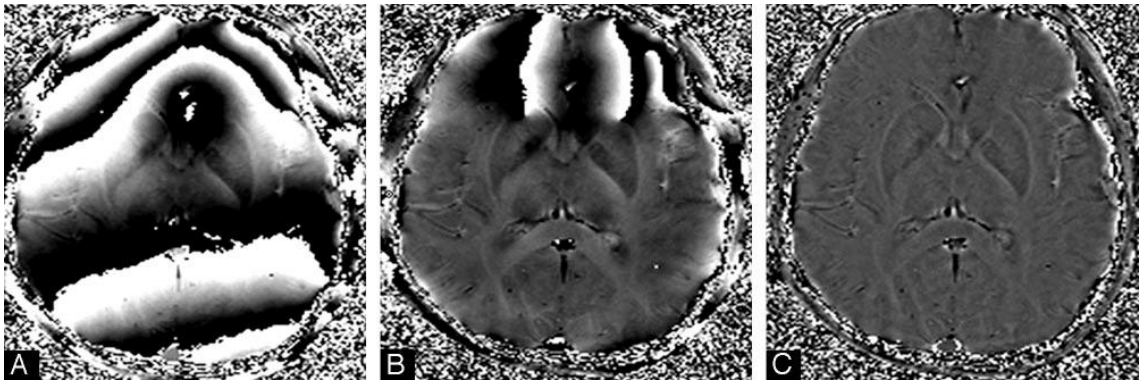

Figure 7.1 A, Phase image. B and C, A filtered with different HP filters (ref. 18)

Figure 7.1 shows that with a filter the tissues with different susceptibilities can be differentiated.

It can be upgraded when combined with magnitude images because phase images are created to suppress pixels with certain values enhancing the image contrast. In other words this is the multiplication between magnitude and phase images.

The phase mask can be negative or positive:

Negative

$$f(x) = \begin{cases} \dfrac{[\varphi(x) + \pi]}{\pi} & , -\pi < \varphi(x) < 0 \\ 1 & , \quad otherwise \end{cases}$$

(46)

The phase with –π will be zero and will grow until zero where the phase takes the maximum value 1.

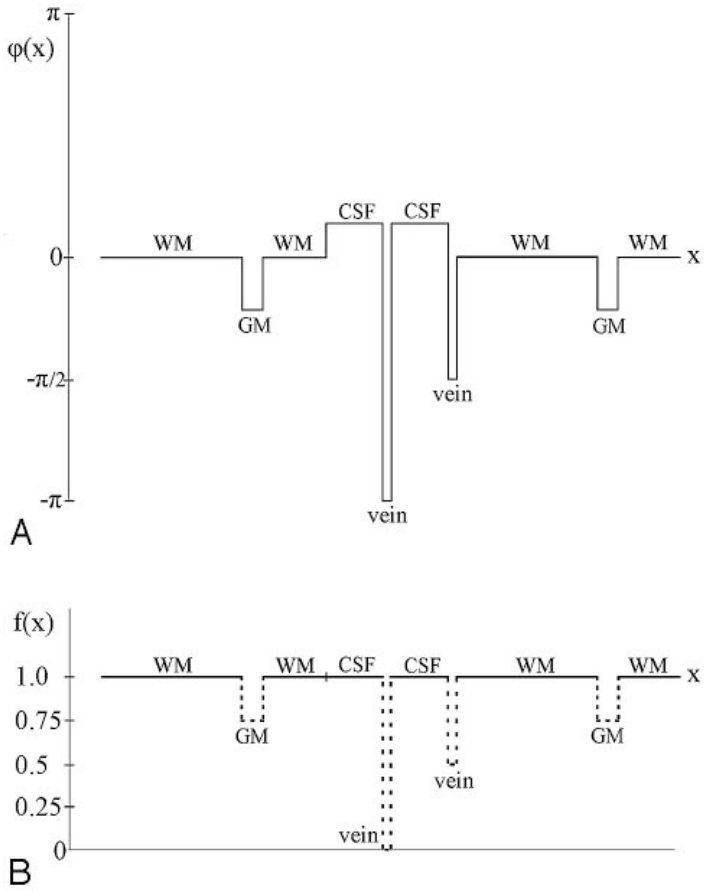

Figure 7.2 Phase mask process. A, phase values of certain tissues. B, negative mask created from A

Positive

$$f(x) = \begin{cases} \dfrac{[\varphi(x) - \pi]}{\pi} & , -\pi < \varphi(x) < 0 \\ 1 & , \quad otherwise \end{cases}$$

(47)

The phase with π will be zero and will grow until zero where the phase takes the maximum value 1.

Where φ(x) is the phase at location x and the limits of the phase of interest are 0 and π or –π are depending on the objective.

If more contrast is required another mask can be made and for this it is only needed to apply to the phase mask the original magnitude image (ρ(x)) as many times as wanted:

$$\rho(x)_n = f^m(x)\rho(x)$$

(48)

The m value represents the number of times that the phase mask will be multiplied to optimize the contrast to noise ratio (CNR) in this case to a point where CNR (m) is maximized.

7.2. Arterial Spin Labeling (ASL)

ASL uses a different tracer than DSC-MRI, in this case magnetic labeled blood water protons are used as an endogenous tracer, meaning a complete non-invasiveness and consequently the possibility of being used in patients with special conditions like kidney failure or in children where the use of exogenous and radioactive tracers are limited, in addition it will permit this technic to be repeated barely without limit.

Besides this, this technic allows perfusion imaging of individual blood vessel of the brain. So with this will be possible to study the blood perfusion, where “perfusion” refers to the delivery of oxygen and nutrients to the tissue. Thus regional changes in tissue functions can be discoverer.

Additionally this technic gives the CBF as an absolute value (ml $100ml^{-1}min^{-1}$).

This technic is based in the production of a labelled image and a control image where the static tissue is the same for both but the inflowing blood magnetization is different. So from the

subtraction control/label is obtained, the signal difference ΔM can be obtained, which reflects to the local perfusion (figure 7.3)

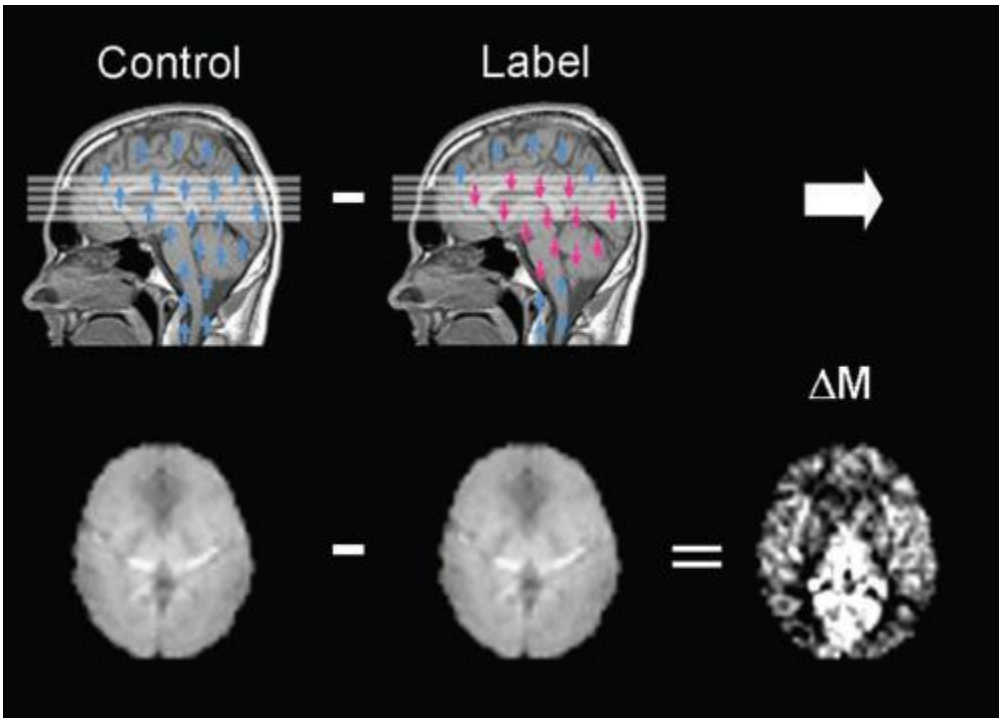

Figure 7.3 ΔM obtained from the subtraction of the labeled images to the control images [37]

The labeling process consists in inverting or saturating water molecules from the blood supplying the imaged region. After this a delay (Inversion delay (TI)) needs to be added so that the labelled blood can reach the capillaries of the region of interest.

This technic is divided in two main groups:

- ***Continuous ASL (CASL)***

This group uses a spatial localized Radio Frequency (RF) to continuously invert or saturate the longitudinal magnetization of the protons from the water of the arterial blood arriving to the brain. The inversion will typically be done proximal to the circle of Willis, nearby the medullospinal junction or at carotid level [37].

Thus the longitudinal magnetization will be reduced on the image slice allowing those images to be subtracted from the control images.

Notwithstanding, it is not a technic without disadvantages, and it can be said that it has three major weaknesses. Firstly there is a large power deposition in tissues from the long labelling

time. Secondly there is a gap between the labelling place and the imaging slices, meaning a that the blood will take some time to travel from one place to another, resulting in increased relaxation before time; in some diseases this time will be too long that the signal from the labelled blood will decay before reaching the tissue. Finally this technic will need non-standard hardware [37][26].

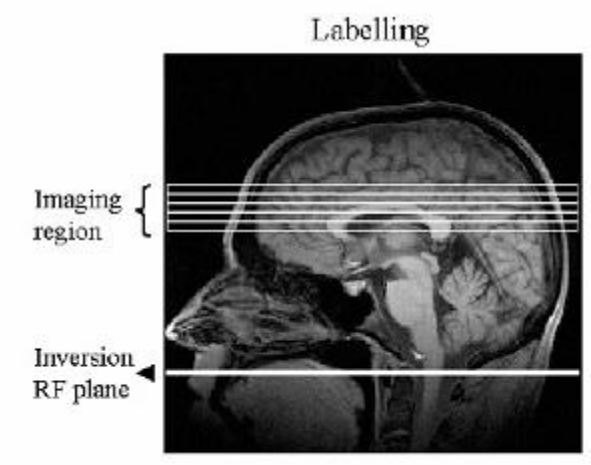

Figure 7.4 blood are inverted in the Inversion Plane and after it flow to the imaging region

- ***Pulsed ASL (PASL)***

This technic uses a large area and a short RF pulse contrary to CASL a continuous inversion over a plain is used.

There are many pulsed technics. For example, in 1994 Edelman et al proposed the EPISTAR (echo planar imaging and signal targeting with alternating radiofrequency). In this technic a single RF pulse of 180^{o} is applied to invert the longitudinal magnetization in a block (10-15cm) below the image slice and the image is taken. In control an inversion slab will be placed superior to the image slice to cancel MT effects [26].

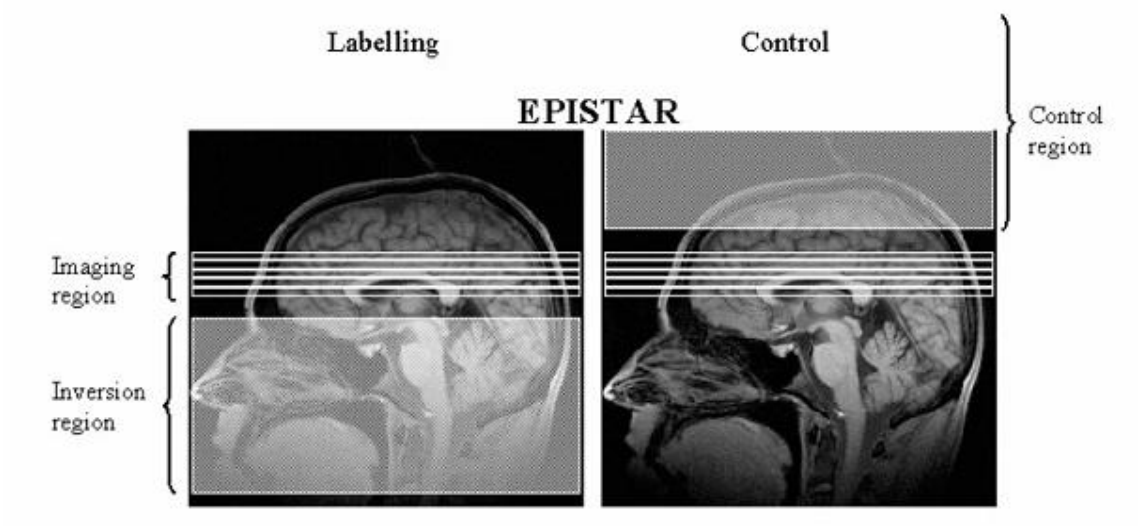

Figure 7.5 EPISTAR technic, shaded areas are the areas covered by the inversion pulse [38]

After this, another proposal arose, by Kim et al., 1995 and Schwarzbauer et all., 1996, one variation called FAIR (flow alternating inversion recovery) involving geometry differences on the inversion slab allowing for contributions of blood flowing from above the slice.

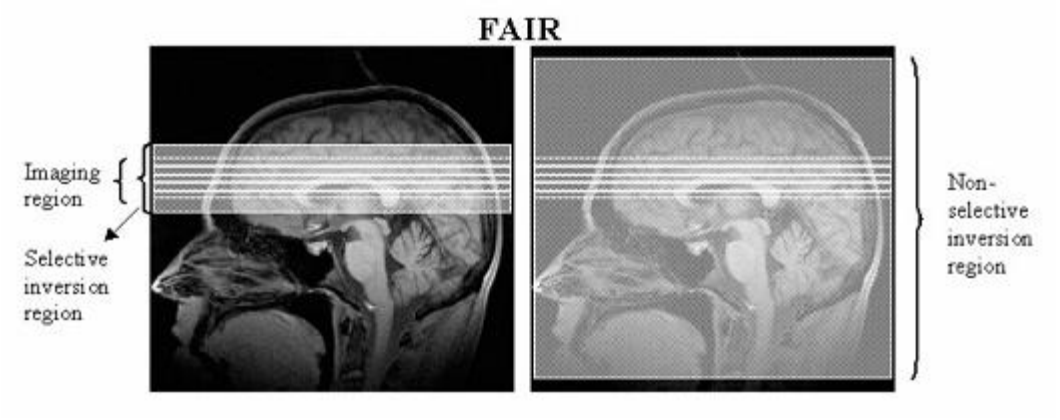

Figure 7.6 FAIR technic [38]

Some others like QUIPSS II (quantitative imaging of perfusion using a single subtraction) or PICORE (proximal inversion with a control for off-resonance effects) have also been proposed.

In the end it can be said that the PASL allows a shortening between the inversion of the arterial spins and the imaging region, improving the efficiency. However a gap of 1-2cm is still needed.

Due to smaller problems and an easier implementation PASL have become more popular for perfusion imaging.

This is only a small review of SWI and ASL, but can give an idea of the huge potential of the both technics.

8. References

1. JEFFRY, R. ALGER, ET AL- *CONTRAST AGENT DOSE EFFECTS IN CEREBRAL DYNAMIC SUSCEPTIBILITY CONTRAST MAGNETIC RESONANCE PERFUSION IMAGING*, J MAGN RESON IMAGING. , 2009
2. JACOB, U.FLUCKIGER, ET AL- *MODEL-BASE BLIND ESTIMATION OF KINETIC PARAMETERS IN DCE-MRI*, MAGN RESON MED. , 2009 , 62(6): 1477–1486
3. BERTOLDO, A., ET AL, *ASSESSMENT OF CEREBRAL BLOOD FLOW, VOLUME, AND MEAN TRANSIT TIME FROM BOLUS-TRACKING MRI IMAGES: THEORY AND PRACTISE. IN ADVANCED IMAGE PROCESSING IN MAGNETIC RESONANCE IMAGING*, ADVANCED IMAGING PROCESSING IN MAGNETIC RESONANCE IMAGING L. LANDINI EDITOR, 2005, CHAP.19, 587-603
4. OSTERGAARD, ET AL- *HIGH RESOLUTION MEASUREMENT OF CEREBRAL BLOOD FLOW USING INTRAVASCULAR TRACER BOLUS PASSAGES. PART I: MATHEMATICAL APPROACH AND STATISTICAL ANALYSIS*, MAGN RESON MED, 1996, 34:555-556
5. OSTERGAARD, ET AL- *HIGH RESOLUTION MEASUREMENT OF CEREBRAL BLOOD FLOW USING INTRAVASCULAR TRACER BOLUS PASSAGES PART II. EXPERIMENTAL COMPARISON AND PRELIMINARY RESULTS*, MAGN RESON, MED, 1996, 36:727-736
6. OSTERGAARD, ET AL- *TRACER ARRIVAL TIMING-INSENSITIVE TECHNIQUE FOR ESTIMATING FLOW IN MR PERFUSION-WEIGHTED IMAGING USING SINGULAR VALUE DECOMPOSITION WITH A BLOCK-CIRCULANT DECONVOLUTION MATRIX*, MAGNETIC RESONANCE IN MEDICINE, 2003, 50:164–174
7. SAKOGLU, UNAL, ET AL- *CEREBRAL BLOOD FLOW ESTIMATION FROM PERFUSION-WEIGHTED MRI USING FT BASED MMSE FILTERING METHOD*, MAGN RESON IMAGING. , 2008, 26(3): 313–322
8. ZAHARCHUK, GREG, ET AL- *IMPROVING DYNAMIC SUSCEPTIBILITY CONTRAST MRI MEASUREMENT OF QUANTITATIVE CEREBRAL BLOOD FLOW USING CORRECTIONS FOR PARTIAL VOLUME AND NONLINEAR CONTRAST RELAXIVITY: A XENON CT COMPARATIVE STUDY*, J MAGN RESON IMAGING. , 2009, 30(4): 743–752
9. LEE, J.J., ET ALL- *DYNAMIC SUSCEPTIBILITY CONTRAST MRI WITH LOCALIZED ARTERIAL INPUT FUNCTIONS*, MAGN RESON MED. , 2010, 63(5): 1305–1314
10. CAVALHEIRO ANA, *ESCLEROSE MULTIPLA* , FARMACIA PORTUGUESA, 1997, VOL 19:33-39
11. KUROIWA, YOSHIGORO, ET AL- *MULTIPLE SCLEROSIS EAST AND WEST : PROCEEDINGS OF THE ASIAN MULTIPLE SCLEROSIS WORKSHOP HELD SEPTEMBER 18-19, 1981, KYOTO, AND PROCEEDINGS OF THE SATELLITE SYMPOSIUM, MULTIPLE SCLEROSIS, 12TH WORLD CONGRESS OF NEUROLOGY HELD SEPTEMBER 23, 1981, KYOTO*, KYUSHU UNIVERSITY PRESS , 1982.

12. BARCELLOS, L. F., ET AL- *HLA-DR2 DOSE EFFECT ON SUSCEPTIBILITY TO MULTIPLE SCLEROSIS AND INFLUENCE ON DISEASE COURSE*, AMERICAN SOCIETY OF HUMAN GENETICS, 2003
13. AMARAL, MANUELA- *ESCLEROSE MULTIPLA E REABILITAÇÃO*, REV. PORT. CLIN GERAL,1995, VOL.12:58-66
14. HTTP://WWW.SISTEMANERVOSO.COM/PAGINA.PHP?SECAO=7&MATERIA_ID=121&MATERIAVER=1, 20-7-2011
15. http://www.websters-online-dictionary.org/definitions/Multiple%20sclerosis?cx=partner-pub-0939450753529744%3Av0qd01-tdlq&cof=FORID%3A9&ie=UTF-8&q=Multiple%20sclerosis&sa=Search#922, 22-7-2011
16. RAUSCHER, ALEXANDER, ET AL- *MAGNETIC SUSCEPTIBILITY-WEIGHTED MR PHASE IMAGING OF THE HUMAN BRAIN*, AJNR AM J NEURORADIOL 26:736–742, 2005
17. HAACKE, E. MARK, ET AL- *SUSCEPTIBILITY WEIGHTED IMAGING (SWI)*, MAGNETIC RESONANCE IN MEDICINE 52:612–618, 2004
18. HAACKE, E.M., ET AL- *SUSCEPTIBILITY-WEIGHTED IMAGING: TECHNICAL ASPECTS AND CLINICAL APPLICATIONS, PART 1*, AJNR AM J NEURORADIOL, 2009, 30:19 –30
19. MITTAL, S., ET AL- *SUSCEPTIBILITY-WEIGHTED IMAGING: TECHNICAL ASPECTS AND CLINICAL APPLICATIONS, PART 2*, AJNR AM J NEURORADIOL, 2009, 30:232–52
20. MCCRORY, DOUGLAS C.- *CRITERIA TO DETERMINE DISABILITY RELATED TO MULTIPLE SCLEROSIS*, AHRQ PUBLICATION, 2004, NO. 04-E019-2
21. HTTP://WWW.MULT-SCLEROSIS.ORG/EXPANDEDDISABILITYSTATUSSCALE.HTML 29-07-2011
22. HTTP://WWW.MULT-SCLEROSIS.ORG/RELAPSINGREMITTINGMULTIPLESCLEROSIS.HTML, 29-07-2011
23. HTTP://WWW.MULT-SCLEROSIS.ORG/MSSTATS.HTML, 29-07-2011
24. HTTP://WWW.MULT-SCLEROSIS.ORG/DIAGNOSINGMS.HTML, 29-07-2011
25. HTTP://WWW.MULT-SCLEROSIS.ORG/MSSYMPTOMS.HTML, 29-07-2011
26. TOFTS, PAUL, ET AL- *QUANTITATIVE MRI OF THE BRAIN: MEASURING CHANGES CAUSED BY DISEASE*, JOHN WILEY & SONS, LTD, 2003
27. HTTP://WEB.NMSU.EDU/~SNSM/CLASSES/CHEM435/LAB8/, 10-08-2011
28. HTTP://WWW.CHEM.UNC.EDU/COURSES/550L/NMR_TUTORIAL/INDEX.HTML, 11-08-2011
29. CASTELLARO, MARCO, ET AL- *STUDIO DELL'EMODINAMICA CEREBRALE IN PAZIENTI AFFETTI DA SCLEROSI MULTIPLA: OTTIMIZZAZIONE DEL PROTOCOLLO DI ACQUISIZIONE E DEL PROCESSO DI QUANTIFICAZIONE*, UNIVERSITÀ DEGLI STUDI DI PADOVA, ITALIA, 2009-2010
30. HTTP://WWW.CIS.RIT.EDU/CLASS/SCHP730/LECT/LECT-9.HTM, 13-08-2011
31. ZANDERIGO, FRANCESCA , *ASSESSMENT OF CEREBRAL HEMODYNAMICS BY DECONVOLUTION WITH DYNAMIC SUSCEPTIBILITY CONTRAST - MAGNETIC RESONANCE IMAGING*, DECEMBER, 2006

32. D. PERUZZO, ET AL.- *AUTOMATIC SELECTION OF ARTERIAL INPUT FUNCTION ON DYNAMIC CONTRAST-ENHANCED MR IMAGES*, COMPUT. METHODS PROGRAMS BIOMED., 2011, DOI:10.1016/J.CMPB.2011.02.012
33. HTTP://WWW.VANDERVEER.ORG.NZ/RESEARCH/LABS/MRI.PHP, 17-08-2011
34. HTTP://MRSRL.STANFORD.EDU/~BRIAN/BLOCH/, 17-08-2011
35. HTTP://WWW.CLEVELANDCLINICMEDED.COM/MEDICALPUBS/DISEASEMANAGEMENT/NEUROLOGY/MULTIPLE_SCLEROSIS/, 17-08-2011
36. POLMAN, CHRIS H., ET AL.- *DIAGNOSTIC CRITERIA FOR MULTIPLE SCLEROSIS: 2005 REVISIONS TO THE "MCDONALD CRITERIA"*, ANN NEUROL 58:840–846, 2005
37. E T PETERSEN, ET AL.- *NON-INVASIVE MEASUREMENT OF PERFUSION: A CRITICAL REVIEW OF ARTERIAL SPIN LABELLING TECHNIQUES*, THE BRITISH JOURNAL OF RADIOLOGY, 2006, 79 688–701
38. HTTP://PHYSICSARCHIVES.COM/INDEX.PHP/COURSES/999, 01-09-2011
39. HTTP://WWW.SPEM.ORG/BIBLIOTECA/DOSSIERS-TECNICOS/204-O-QUE-E-A-ESCALA-EDSS, 01-09-2011
40. HTTP://WWW.MEDIMAGINGSALES.COM/MEDICAL-IMAGING-EQUIPMENT/MRI/PHILIPS/PHILIPS-ACHIEVA-1-5-T-A-SERIES-MRI,01-09-2011